8-2013

Network Dynamics of Visual Naming

Christopher R. Conner

NETWORK DYNAMICS OF VISUAL NAMING

By

Christopher Richard Conner, B.A.

Committee:

Nitin Tandon, M.D.
Supervisory Professor

Harel Shouval, Ph.D.

Valentin Dragoi, Ph.D.

Steve Cox, Ph.D.

Edgar T Walters, Ph.D.

Arne Ekstrom, Ph.D.

Dean, The University of Texas
Graduate School of Biomedical Sciences

NETWORK DYNAMICS OF VISUAL NAMING

Presented to the Faculty of The University of Texas Health Science Center at Houston and The University of Texas M. D. Anderson Cancer Center

Graduate School of Biomedical Sciences

in Partial Fulfillment

of the Requirements

for the Degree of

DOCTOR OF PHILOSOPHY

By

Christopher Richard Conner, B.A., Houston, Texas

August, 2013

DEDICATION

This thesis is dedicated to my graduate school cheerleader, Chelsea.

ACKNOWLEDGEMENTS

I would like to thank my supervisory professor, Nitin Tandon, for providing both scientific and clinical mentorship over the last six years. Thanks to everyone in the lab (Tom Pieters, Vatche Baboyan, Cihan Kadipasoglu, Mike DiSano, Megan Whaley) for helping out with experiments.

I want thank all the faculty that served on my advisory, examining and supervisory committees and for giving me valuable feedback during my development. Thanks to Edgar T Walters, Valentin Dragoi, Harel Shouval, Steve Cox, Arne Ekstrom, Andrew Bean, Hongzhen Hu, Michael Beierlein, Patrick Dougherty, Jeff Actor, and Tim Ellmore.

I would like to thank my funding sources: the Keck Center of the Gulf Coast Consortia for my grant for Training in Theoretical and Computational Neuroscience from the National Institute of Biomedical Imaging and Bioengineering (NIBIB) (T32EB006350) and University of Texas Board of Regents for a fellowship from the Graduate Student Initiative.

I'd like to thank everyone who is a part of the MD/PhD program here at UT Houston including my program mentor Ruth Heidelberger, all the directors, and Dianna Milewicz. Special thanks to Jo Cheatwood for helping me navigate through the whole program. To Nick, Brandon, David, Javier and everyone else who understands what it is like to see all of your medical school class move on while you're stuck in grad school.

Finally, I owe a huge debt of gratitude to my family. Mom and Dad for knowing when to give tough love. To my grandparents for inspiring me. To Katie

and Tim for laughing about grad school. And of course to my girlfriend, Chelsea, for enduring five years of long distance dating and more complaining than everyone else combined.

ABSTRACT

NETWORK DYNAMICS OF VISUAL NAMING

Publication No._____

Christopher Richard Conner, B.A.

Supervisory Professor: Nitin Tandon, M.D.

Recognition and naming of objects and actions are fundamental components of language. They involve several different systems working in coordination to accomplish a complex behavior. During visual naming, sensory and semantic processing are carried out by dedicated cortical substrates in the temporal and occipital lobes, while response selection and articulatory planning are handled by prefrontal cortex. Despite decades of research using lesion analysis, functional MRI and electro-encephalography, the precise dynamics involved remain unknown due to the inadequate spatio-temporal resolution of these methodologies. Of particular interest is the organization of semantic knowledge and the degree of serial and parallel organization of the language production system. To better understand these issues, we studied epilepsy patients undergoing electro-corticography during visual naming of nouns and verbs. Employing novel methods for grouped data analysis, we found that initial processing concurrently activated ventral temporo-occipital cortex, which implies that this level of semantic processing occurs in parallel. However, we found significant differences, both in extent and location, between

noun and verb processing in the visual ventral (noun) and dorsal (verb) processing streams. This suggests that slightly different networks are involved in the storage and retrieval of separate grammatical categories. To characterize subsequent activity within prefrontal cortex, we used measures of information flow to investigate the network dynamics of speech production. Unlike sensory processing, we found distinct processing stages during which separate operations are executed in parallel. Specifically, pars orbitalis of left inferior frontal gyrus controlled the onset of response selection and phonological planning, which were executed at the same time. Processing was subsequently terminated through ascending input from motor cortex. The interplay of these control signals, both ascending and descending, resulted in distinct state transitions, implying a degree of seriality to speech production following the parallelism of semantic retrieval. The differences in processing architecture between retrieval and articulation are possibly related to the dissociations of function – memory storage and access are largely associative, whereas motor actions are tightly controlled over time.

TABLE OF CONTENTS

DEDICATION iii

ACKNOWLEDGEMENTS iv

ABSTRACT vi

LIST OF TABLES x

LIST OF FIGURES xi

LIST OF ABBREVIATIONS xiv

CHAPTER 1: INTRODUCTION 1

The Mental Lexicon 2

Modeling Speech Production 7

Functions of Broca's Area 13

Goals 16

CHAPTER 2: DISSOCIATING NOUN AND VERB NAMING 18

Introduction 19

Methods 22

Results 30

Limitations 38

Conclusions 39

CHAPTER 3: INFORMATION FLOW WITHIN BROCA'S AREA 42

Introduction 43

Methods 45
Results 48
Conclusions 62
Limitations and Alternative Explanations 66
CHAPTER 4: CONCLUSION 72
Significance 75
Future Directions 76
Summary 78
APPENDIX: Amplitude Envelope Correlations 81
Equations 81
Simulations 83
Application 85
REFERENCES 87
VITA 108

LIST OF TABLES

Table 2.1 Summary of patient demographics 23

Table 2.2 Spatial coordinates of peak activation sites 37

LIST OF FIGURES

Figure 1.1 Hierarchical network model 4

Figure 1.2 Schematic of the spreading activation model 5

Figure 1.3 Cell assemblies as nodes 6

Figure 1.4 Parallel distributed model 9

Figure 1.5 Levelt-Roelefs-Meyer model 12

Figure 1.6 Anatomy of Left Inferior Frontal Gyrus 14

Figure 1.7 Controlled retrieval and response selection 16

Figure 2.1 Task design and overview of analysis 24

Figure 2.2 Distribution of electrodes used in the analysis 25

Figure 2.3 Verb and noun naming contrasted with scrambled images 31

Figure 2.4 Group verb minus noun naming and conjunction analysis 32

Figure 2.5 Single subject ECoG analysis 33

Figure 2.6 Average time series for regions with significant activation 34

Figure 2.7 Grouped analysis of fMRI data 36

Figure 3.1 Task design and methods overview 47

Figure 3.2 Reaction times for each condition 48

Figure 3.3 Time-frequency analysis of noun naming 50

Figure 3.4 Time-frequency results of verb and scramble naming 51

Figure 3.5 Gamma power changes of nouns based on word frequency 52

Figure 3.6 Time-frequency analysis of right hemisphere SDEs 53

Figure 3.7 Single subject AEC results during noun naming 55

Figure 3.8 Functional connectivity of left IFG during noun naming 56

Figure 3.9 Functional connectivity of left IFG during verb naming 57

Figure 3.10 Functional connectivity of left IFG during scramble naming 58

Figure 3.11 LIFG dynamics of functional connectivity during noun naming 60

Figure 3.12 LIFG temporal dynamics during verb and scramble naming 61

Figure 3.13 Attractor state model for noun naming 64

Figure 3.14 Two possible explanation of observed negative correlations 68

Figure Appx.1 Zero lag connectivity 84

Figure Appx.2 Weak connectivity 84

Figure Appx.3 Lagged connectivity 85

Figure Appx.4 Filter design 86

LIST OF ABBREVIATIONS

AEC	Amplitude Envelope Correlation
BA	Brodmann Area
CSM	Cortical Stimulation Mapping
DLPFC	Dorso-lateral Prefrontal Cortex
ECoG	Electro-corticography
FDR	False Detection Rate
FFT	Fast Fourier Transform
fMRI	functional Magnetic Resonance Imaging
IQ	Intelligence Quotient
ITG	Inferior Temporal Gyrus
LI	Laterality Index
(L)IFG	(Left) Inferior Frontal Gyrus
LFP	Local Field Potential
LRM	Levelt-Roelfs-Meyer model
M1	Primary Motor Cortex
MEMA	Mixed Effects Multilevel Analysis
MNI	Montreal Neurological Institute
PDP	Parallel Distributed Processing
PHG	Parahippocampal Gyrus
POp	Pars Opercularis
POr	Pars Orbitalis
PT	Pars Triangularis

SDE	Subdural Electrode
SFG	Superior Frontal Gyrus
SLOC	Superior Lateral Occipital Cortex
STG	Superior Temporal Gyrus
VLPFC	Ventro-lateral Prefrontal Cortex

CHAPTER 1: INTRODUCTION

Language is a complex behavior central to human psychology. Despite a century and a half of intense study, modern understanding of language lacks answers to several fundamental questions of neuro-linguistics. These include the organization of lexico-semantic knowledge and the structure and order of processing. Such deficits are driven by the lack of an appropriate animal model and the use of methods with inadequate spatio-temporal resolution to study the underlying neural dynamics. Nevertheless, several theories have been developed as a result of the lesion and neuro-imaging studies that have been performed. However, given the limitations of these techniques, there is substantial opportunity for novel approaches to test existing models of language (1).

Historically, advances in linguistics can be divided broadly into three components: [1] the study of how words and their semantics are stored, [2] the means by which these words are produced, and [3] the actions of prefrontal cortex to control the underlying processes. To some extent, the development of theory regarding them has followed this order and began with the mental lexicon, the means of storing vocabulary.

The Mental Lexicon

The core function of speech is the ability to retrieve words from memory and articulate them. This process is referred to as binding word and form (2), and it often involves processing of sensory information followed by accessing the 'mental lexicon' (3-5). This structure has been thought to encompass all the words that a person has access to, stored in a dictionary-like repository (6). The idea that the mental lexicon exists as a single list was initially used as a means of computational

modeling (7). Entries in the lexicon were thought to be sorted by frequency of use; an ordering that accounts for the faster retrieval of more commonly used words. This model implies that the mental lexicon would be the same for each individual, as it was based around a single, logical rule for indexing. However, there were two notable issues with this premise: retrieval from a list usually requires a sequential search mechanism (8), and it was unclear what information would be stored along with each entry.

Subsequently, the hierarchical network model was developed with the idea that words should be stored according to their semantics (9). In this schema, words are arranged in a tiered taxonomy, with parent levels describing a class (“animal”) and subordinate levels representing its members (“mammal”, “lizard”). Retrieval of words involves traversing down the tree until the search reaches a terminal point at end of a branch (Figure 1.1). The depth of the tree that must be covered determines the speed of this process and is referred to as the semantic distance. The implementation of a branch-decision method was more efficient than a simple list in terms of both storage and retrieval. It also introduced the idea that knowledge about a word would be related to its relationships with other words, and could be inferred by such connections. However, the central idea that the speed of operations was dependent on semantic distance was not validated. For example, in a sentence falsification task the phrase “a dachshund is a mammal” has a shorter semantic distance than “a dachshund is a fruit”, but subjects are able to reject the second sentence more quickly (10). This problem was due to the sparse storage of information associated with each word. Each feature about a class was stored once

and then inherited by all members. The semantic distance between a word and the fundamental concepts related to it (e.g. a dachshund is an animal) was still too large.

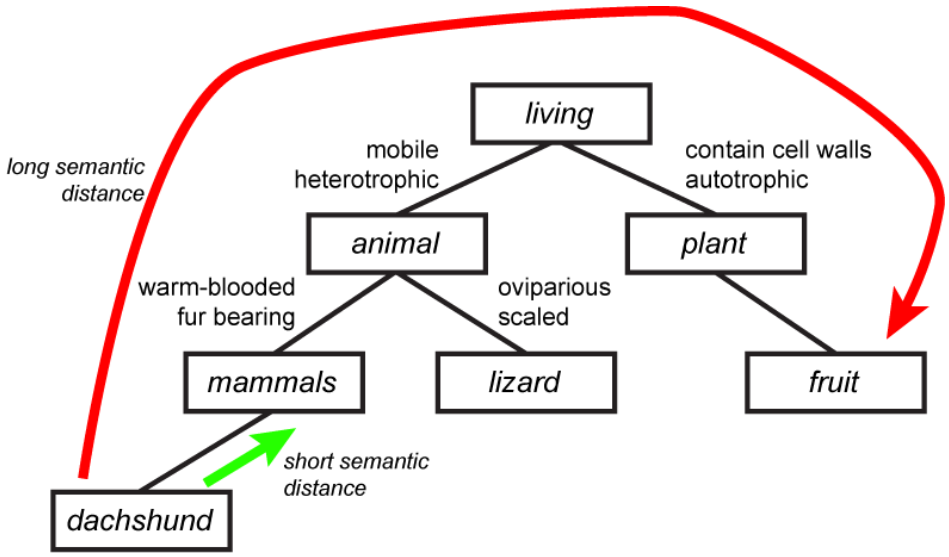

Figure 1.1 Hierarchical network model
Each word is arranged according a semantic hierarchy. At each branch point of the tree there are multiple options, with different semantic features associated with each branch. All nodes beneath a certain point inherit the features above that point. During word retrieval, the search begins at the top of the tree and moves down. The semantic distance is defined as the total depth of traversal between any two points. Accessing semantic information for a given word involves traversing up to the tree until the desired information is obtained. Shown is the semantic distance for validating "a dachshund is a mammal" and "a dachshund is a fruit".

In order to maintain storage efficiency while decreasing semantic distance, the branching architecture was replaced with a network representation known as the spreading activation model (11-16). Under this framework, words are represented as the nodes of a graph and are activated either by sensory cortices processing external stimuli; or internal goal-oriented cortex responsible for executive function (17, 18). Input is fed into a node, increasing the level of activation, which then spreads to its neighbors (related words and concepts) (Figure 1.2). Unlike the hierarchical model, relationships between words are handled via the network topology and any pair of words can be directly connected, allowing the

semantic distance to decrease dramatically. Such a representation is appealing because it leverages the associative structure of memory (19, 20). Furthermore, it accounts for the phenomena of semantic priming, which is observed by cuing a subject with a related word before having them name a subsequent target stimulus (e.g. “dog” followed by “cat).

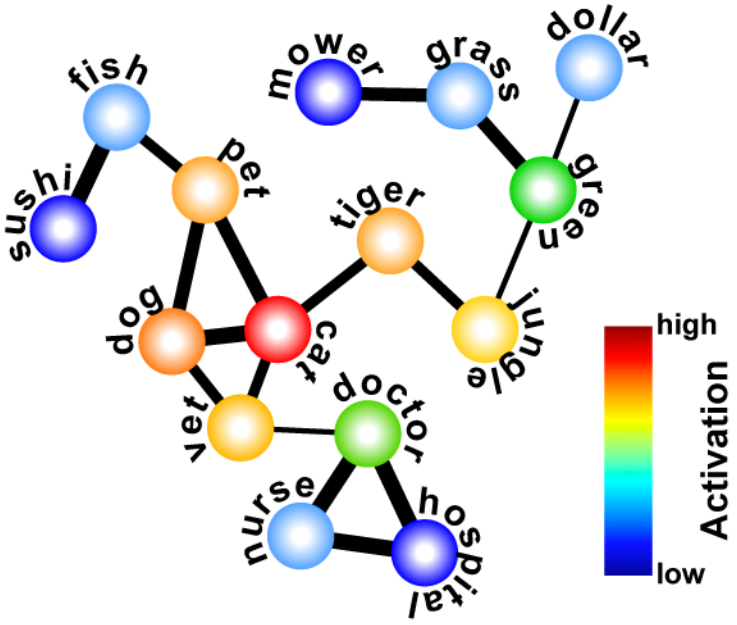

Figure 1.2 Schematic of the spreading activation model
Each node represents a separate entry into the mental lexicon. The edge between each pair of node denotes the strength of semantic inter-relatedness. The node with the highest activation (here it is “*cat*”) is the node that is retrieved. Words that are similar semantically also receive activation, but ultimately do not reach threshold and are not retrieved.

Implementation of the spreading activation model utilizes Hebbian learning rules for organization (21, 22) (Figure 1.3). Each word-node is a collection of cells that respond to semantic features of a stimulus. The greater the number of features present, the greater the overall firing of neurons within the assembly. This is in contrast to previous models that worked using rigid logic for classification, which implied that all individuals have an identical structure for their mental lexicon. Spreading activation, on the other hand, results in organization that is highly

idiosyncratic and would lead to novel associations for each individual (4, 7, 15, 16, 20, 23-27). Unfortunately, this makes the model extremely difficult to falsify due to the lack of predictions that it makes. Nevertheless, it has become the dominant model of the mental lexicon due to its pure implementation through simple learning rules.

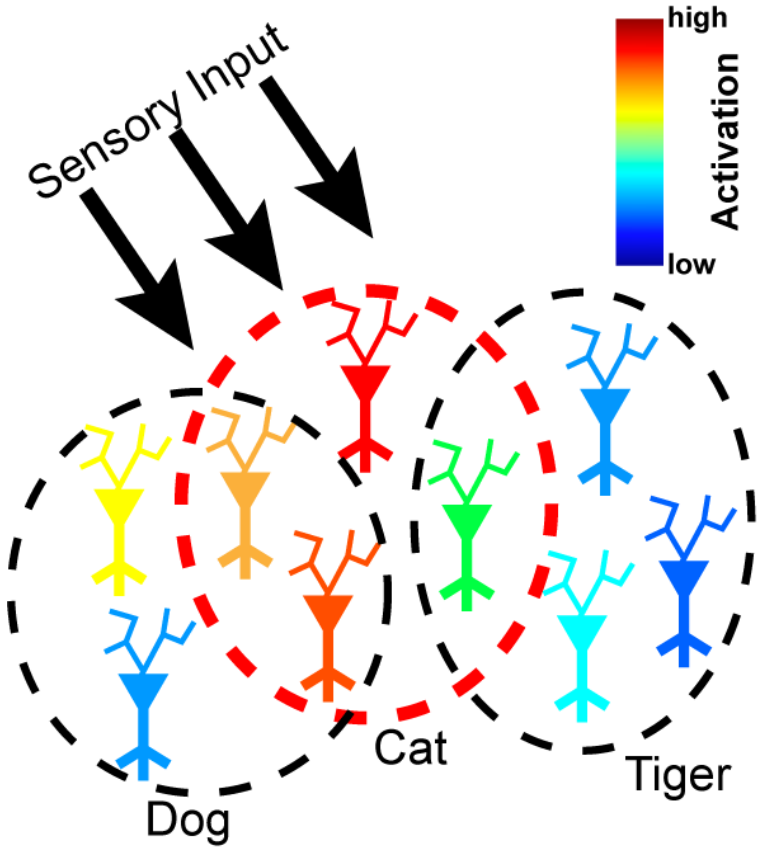

Figure 1.3 Cell assemblies as nodes
Nodes within the spreading activation model are implemented as connected cell assemblies. Each cell codes for a separate semantic feature, and overlap between related words are handled by neurons shared by the assemblies. The cell assembly with the greatest activation is the word that is retrieved (the word "cat" is retrieved in this case).

One corollary to this theory is that any area of cortex could become associated with language, given that its role in cognition has a ready, linguistic analogue. Perhaps the best example of this is the possible involvement of primary motor and parietal cortex in the selective processing action words and verbs. This

idea, referred to as the motor theory of language (20, 28-31) or the embodied cognition hypothesis (23, 32-35), stipulates that during both production and recall of such words that these cortices are involved in semantic processing and lexical access. For instance, when asked to name a picture of a person running, leg motor cortex becomes active in part due to mirror neuron activation and mental rehearsal. These regions then assist more traditional language cortices with their lexical processing by incorporating themselves into the distributed cell assembly associated with the word for “running”. This theory provides a testable hypothesis, that nouns and verbs are dissociated both grammatically and in terms of where they are stored in the brain. Initial neuroimaging and lesion studies of the differences between naming animals and tools initially held promise that there may be dissociation between grammatical classes (36-38). However, more recent results have been inconclusive and even contradictory, highlighting the need for more investigation on dissociation of grammatical classes.

Modeling Speech Production

As models of word storage became more developed, the focus began to shift towards speech production. Two general classes of models drew attention, although they were designed to account for separate behavioral phenomena. The first class grew out of the spreading activation model for the mental lexicon by adding a simple layer for phonology onto this existing architecture. These models, best represented by Dell’s connectionist model, were largely based on common speech errors and the consequences of injury to brain tissue involved in language (11, 25, 26, 39). As they incorporated the principles of spreading activation, these models are best

described as implementing non-modular parallel distributed processing. The second class of models was based around the use of chronometric studies of language generation. Their development relied heavily on additive factors logic, which assumes that a certain degree of linear, time-invariant processing occurs in speech production (4, 5, 14-17, 40). As a result, their structure is serial and highly modular. The Levelt-Roelfs-Meyer (LRM) model, a representative member of this class, incorporates six levels of processing that operate in sequence to achieve articulation. The differences between these classes of models represent a major debate within linguistics over the degree of parallelism or seriality in speech production.

Parallel distributed processing models rose as an extension of the spreading activation. Utilizing a degree of pattern selection, they match input features to words, which then connect to phonemes and syllables (13, 41, 42). In many cases, these theories are able to incorporate several different types of stimulus input – including orthography, phonology, and visual processing; into a single model (41-44). Activation is allowed to flow between levels in both feedforward and feedbackward directions, causing the different levels of the system to integrate with each other. Input is fed into the feature layer, where nodes represent large details of the observed stimulus (Figure 1.4). This could include letters for an orthographic stimulus, syllables for an auditory stimulus, or components of form for a visual stimulus (e.g. the concept of “stripes” when seeing a tiger or a zebra). The activation of this level begins to stimulate the second level where nodes are entries in the mental lexicon. Nodes in the second level (representing lexemes – single

entries in the lexicon representing words) increase in activity as a greater number of connected feature nodes are stimulated, until a single response is chosen. In order to limit the number of activated nodes, some models began to incorporate lateral inhibition as a means of narrowing the final output to a single response (45-47). In this way, nodes were able to shut down competitors that may share many relevant features and minimize the number of speech errors. Finally, each lexeme is connected to the sounds and motor commands that comprise its articulation. Once these nodes are activated, the processing is complete.

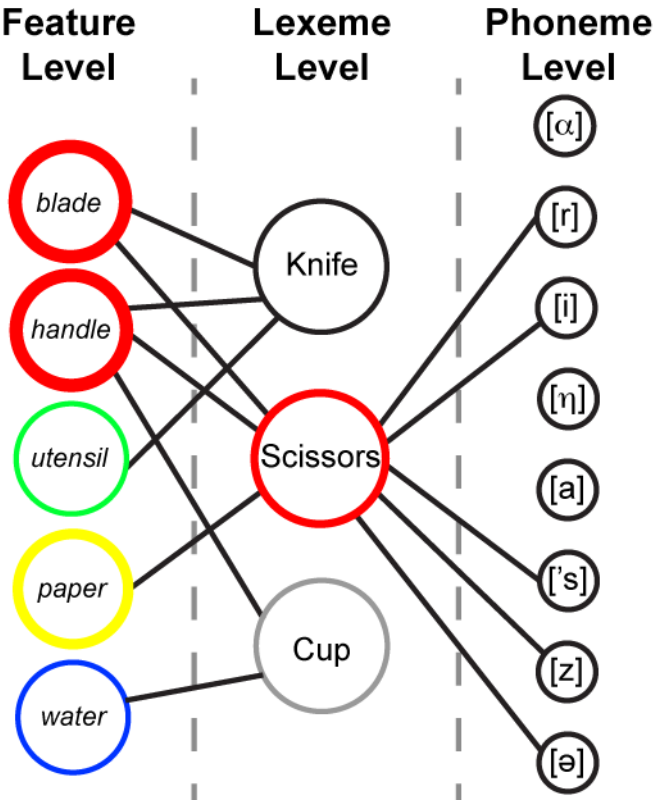

Figure 1.4 Parallel distributed model
Three layers of processing are used: a semantic feature level, a lexeme or word level, and the phonological output level. The dynamics of this model are similar to the spreading activation model for the mental lexicon. Input increases activation of semantic features that spread to the word level. Once a word reaches the activation threshold, it drives the phonologic level that results in speech output. In this case, the stimulus is a picture of scissors, which activates the related features. The lexeme *scissors* is selected and its attached phonemes are chosen.

The parallel distributed model succeeded in the goal of accounting for deficits after damage to the cortex and for the most common speech errors. Notably, this model demonstrated how the lexical bias effect could occur in common speech. This error occurs when one word is replaced by another complete word that is related to the intended lexeme. The bias is towards words that exist and the speaker knows, as opposed to neologisms (novel words devoid of meaning). The connectionist model could also account for selective deficits that impaired retrieval of whole categories of words after brain injury (48, 49) via insult to both the feature and lexeme levels. However, the ability of the connectionist model to successfully account for some observed behavior was at odds with the poor representation of timing in the system and the need to incorporate grammar and syntax. There is no mechanism for control of the system, and without some timing mechanism the retrieval of more than one word can quickly lead to significant errors.

In contrast to the parallel distributed model, several models were investigated that attempted to account for the serial nature of speech (4, 15, 17, 19). As a result, many of these models were designed around fluent sentence production, which requires a tighter control of timing than single word generation accounted for in many of the parallel models. One example of this class is known as the Levelt-Roelefs-Meyer (LRM) model. Processing in this model begins with initial activation of lexical concepts (Figure 1.5). This processing stage is similar to the feature and lexeme processing levels of the connectionist model. However, it differs in that subsequent processing does not occur until the operations of this stage are complete. These concepts are connected to the next stratum that contains lemmas

– the canonical or root form of each word that comprises the entry in the mental lexicon. Multiple lexical concepts can feed into a single lemma, as long as they are derivatives of the same root. For example, “*throw*”, “*throwing*”, and “*threw*” would all feed into the same lemma “TO THROW”, as they are conjugates of that infinitive. Importantly, these lemmas are shared across input modalities and could be activated by auditory, pictographic and orthographic stimuli. Attached to each lemma are elements of syntax and grammar that are necessary for using that word. After this stage, a single word is selected (the process of lexical selection) and prepared for articulation. In subsequent steps, the phonology of the word is retrieved, and these phonemes are assembled into syllables that are used to generate the motor plan. These models diverge from the connectionist one in that at several points (lexical concept, response selection, articulatory planning) processing may not be allowed to progress until that stage is complete. Further, while some levels may send feedback to earlier processing stages, this is not universal. Both of these features are consequences of the desire to have a serial order of processing that could be described by a linear progression of lexical access and speech planning.

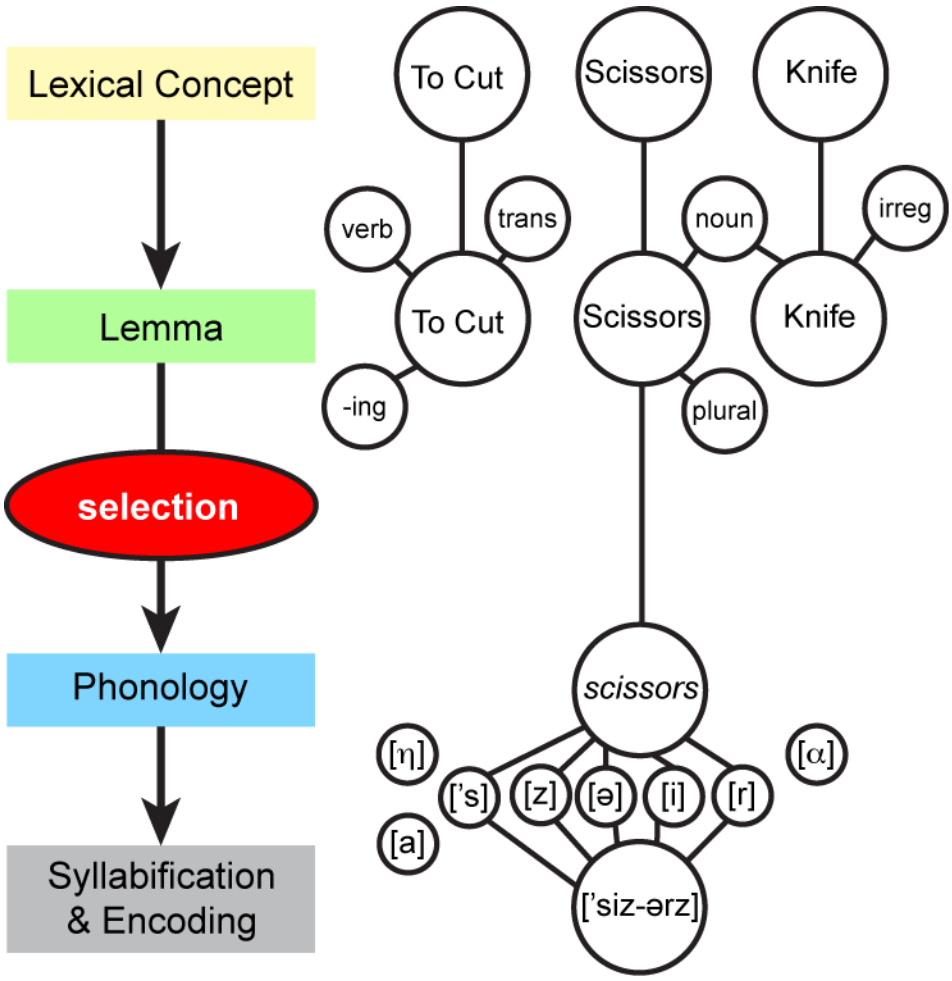

Figure 1.5 Levelt-Roelefs-Meyer model
Lexical access proceeds via spreading activation and results in the activation of several lexical concepts. The activation of these concepts is fed into the lemma layer, which contains the entries in the mental lexicon. This layer contains all relevant syntactic and grammatical information for each entry, but no semantic information. Only one lemma is selected and activates the form layers where phonemes are assembled into complete syllables for encoding and motor planning.

Serial models of language production rely on a degree of modularity not present in the parallel models. These models assume that lemmas are shared by all language-processing streams, and that they co-localize with syntactic information. However, at this time there is little functional evidence for the existence of the lemma (14). Even more problematic is the finding that patients with brain damage can have grammatical deficits that are selective for different streams of language input and production – strongly implying that there is no such shared representation.

It is also possible for patients to generate speech errors (incorrect word selection, errors in articulation) with selective modalities. Both of these observations are not be possible under this formulation of lemma. Regardless of whether lemma is a component of language processing, these models make the prediction that activation in the brain will proceed in discrete stages. This includes the ordering of semantic processing and response selection prior to phonological encoding. Given the importance of seriality and limited feedback between levels, testing this hypothesis is reliant on a method with high enough temporal resolution to investigate the network dynamics underlying these processes.

Functions of Broca's Area

Many of the functions described in these models are attributed to a region of left prefrontal cortex known as Broca's area (the left inferior frontal gyrus, LIFG). This region, first described in 1861 by Paul Broca, is commonly sub-divided into into anatomically distinct sub-regions: pars opercularis (POp; Brodmann Area 44), pars triangularis (PT; BA45) and pars orbitalis (POr; BA47/10) (50, 51) (Figure 1.6). Studies of cytoarchitectonics and receptor density of these regions has revealed significant differences between them (52, 53). These include the presence of an external granular cell layer in PT, while POp and primary motor cortex (M1) are agranular and POr is dysgranular. Further, studies of receptor concentration with cortex have led to increased parcellation of these regions based on differences in concentration of GABA, AMPA or metabotropic receptors. This diversity strongly suggests that the function of LIFG sub-regions is heterogeneous and requires

methods with high spatial resolution in order to character their role in language production.

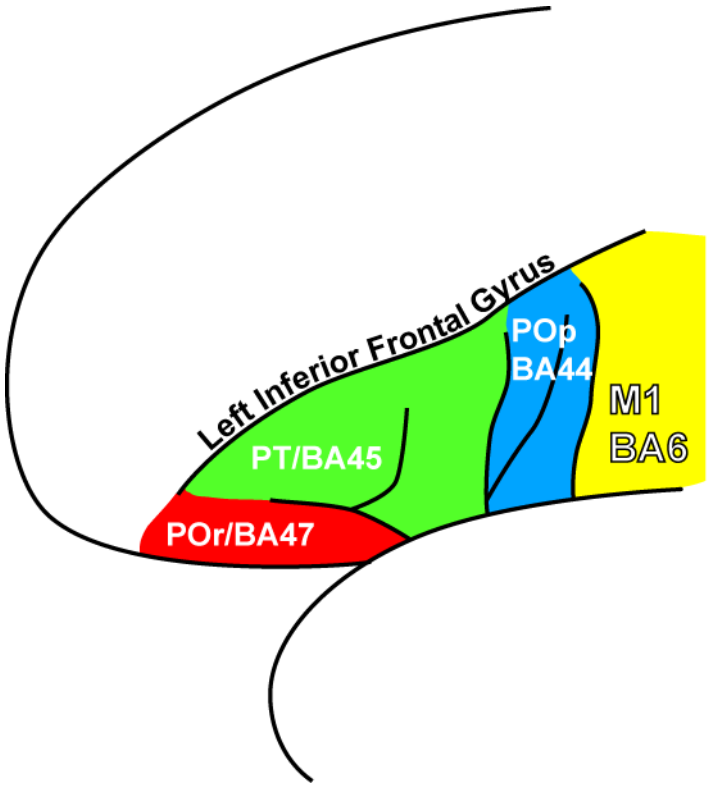

Figure 1.6 Anatomy of Left Inferior Frontal Gyrus
Left Inferior frontal gyrus is commonly divided into 3 sub-regions: pars orbitalis (POr, Brodmann Area 47), pars triangularis (PT, BA45) and pars opercularis (POp, BA44). It is bordered posteriorly by primary motor cortex (M1, BA6).

Given the importance of Broca's area in speech production, several frameworks for function of the LIFG have been developed to explain its role in language. Studies of patients with selective lesions to POr and PT, and fMRI of health subjects have investigated the processes of controlled retrieval and response selection (54-56). The two-process theory incorporates both of these operations into a single paradigm wherein POr is thought to assist semantic processing in association cortex via top-down activation (known as controlled retrieval), while PT uses competitive dynamics and lateral inhibition to choose the final word for articulation (response selection) (16, 45-47, 57) (Figure 1.7). However, an

alternative to mechanism for controlled retrieval is inhibition of response selection (58), which would allow semantic processing to progress prior to lateral inhibition. Distinguishing between these implementations is not feasible using neuroimaging because it requires high spatio-temporal resolution for information flow analysis, but would be possible using intracranial electro-encephalography (ECoG).

In addition to response selection, the domain specific (59, 60) and domain general models (61, 62) offer alternative views on additional PT functionality and its role in phonologic processes. The domain specific model stipulates that PT is only involved in semantic operations (e.g. response selection) while POp alone completes phonologic processing. On the other hand, the domain general model asserts that PT is involved in these processes. Distinguishing between them would require a handful of tasks with varying degrees of response selection and phonological demands to determine if PT is selectivity involved in semantics or has further involvement with phonology. Finally, in the context of the serial models of speech production, several authors have argued for the existence of a classic control hierarchy within the LIFG. This paradigm requires anterior regions to control and co-ordinate activity within posterior regions, with the flow of information is in a rostro-caudal gradient (63-66). POr or PT would act as a mechanism for controlling processing POp and M1, possibly via feedforward inhibition. If the structure is truly hierarchical, this processing will not be reciprocated. As with the two-process theory, validation of this structure will require studies of information flow that cannot be carried out with existent datasets.

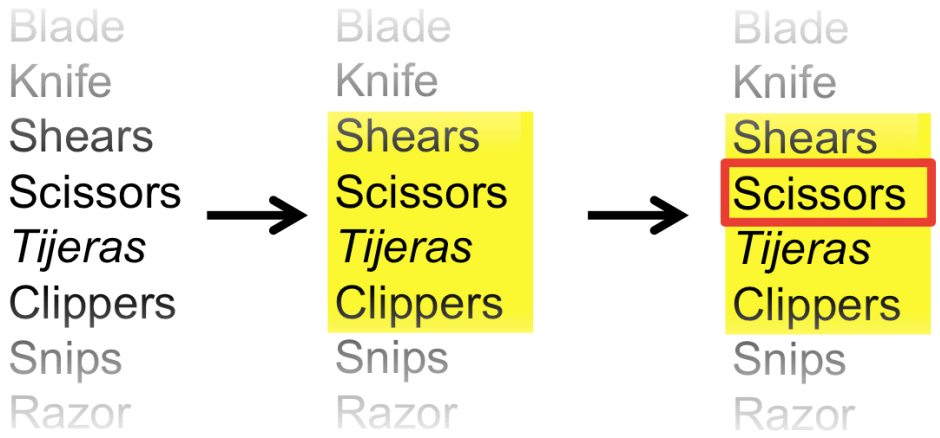

Figure 1.7 Controlled retrieval and response selection
In the two process model of LIFG, controlled retrieval and response selection are executed by prefrontal cortex. Initially, several responses are possible given a stimulus (first column). Controlled retrieval results in activation bias during lexical access, which assists some of these nodes in achieving the threshold for output (shown here as a yellow box around possible outputs). If several responses are near threshold, one must be isolated for output, this is the process of response selection (the red outline in the third column).

Goals

Unfortunately, current studies have been unable to address many of these pressing questions (67). This is partially due to the distributed nature of language processing (1, 68), but is largely a result of the methods available for studying language in humans. One promising avenue to re-examine these issues is the use of invasive electrophysiology, a technique with extremely high spatio-temporal resolution. Using these data, we have worked to address three unresolved debates in the field of neurolinguistics.

1. First, are there significant distinctions between the storage of nouns and verbs across the cortex? As discussed, there remains open debate within the neuroimaging and lesion literature as to whether these different grammatical classes are processed using the same neural substrates. Answering this question would provide insight into the organization of the mental lexicon and would settle discussion

over the spreading activation model. **Our hypothesis was that that the differences between nouns and verbs would largely be within the inferior temporo-occiptal cortex (favoring nouns), and the lateral parietal and motor cortices (favoring verbs) – the dual stream hypothesis.**

2. Second, there are several frameworks describing the functions of Broca's area and the remaining LIFG, although it is well established that this region is crucially important in language production. We sought to find the regions involved in response selection and controlled retrieval, and investigate the functional hierarchy of this region. **Our hypothesis was that these two processes would be an emergent property of the functional connectivity between LIFG sub-regions, and that this area would not follow a rigid hierarchy, but would process language in parallel.**
3. Third, the degree to which processing within the mental lexicon and the LIFG is serial or parallel remains an important distinction between the major classes of speech production models. **Our hypothesis was that speech production at all levels would not proceed serially (in stages), but would be characterized by the spreading activation model during both lexical access and speech production.**

CHAPTER 2: DISSOCIATING NOUN AND VERB NAMING

Introduction

The spreading activation model stipulates that the storage of words involves formation of distributed cell assemblies with each constituent neuron coding for a relevant semantic feature (21, 22). The implication of this is that words with similar meanings would share significant portions of their cell assemblies. Testing of this hypothesis was carried out by investing the activation profiles of two distinct grammatical classes: nouns (animals, tools, faces, places) (23, 37, 49, 69-72) and verbs (48, 73-78). Historically this hypothesis has been tested using studies of patients with lesions or in healthy subjects using neuroimaging modalities. However, the distinctions between these word categories may occur at short time scales that are not resolvable using these methodologies. This is issue is evident in the disagreement between lesion and fMRI studies over the possible differences between noun and verb naming.

The debate over grammatical classes motivated the first goal of our work, to examine the spatial and temporal dissociations of nouns and verbs. Our hypothesis was that there would be differences between these classes and such distinctions would be in agreement with the dual stream hypothesis (79) and the motor theory of language (31). Specifically, noun recall would preferentially activation inferior temporo-occiptal cortex, while verb naming would recruit the lateral parietal and motor cortices. If true, these findings would offer some support to the spreading activation model and its associative structure for the mental lexicon.

Additionally, the high temporal resolution of ECoG data also allow for precise chronometric studies of cortical processing. In the third goal, we sought to examine

the serial or parallel structure of processes involved in word production. Our initial hypothesis was that production at all levels would not proceed serially, but would be characterized by the concurrent activation of the regions involved in lexical access and speech production. Approaching this problem using only the temporal activation profiles would offer some insight into debate.

To test these assertions, we collected intracranial ECoG data using subdural macro electrodes. Given the unique spatio-temporal characteristics of this dataset, it is possible to evaluate the hi-speed, transient interactions that are inherent to language generation (68, 78, 80, 81). However, two major issues with ECoG are inter-subject variability and limited electrode coverage per individual (a “sparse sampling” issue). These problems are compounded by varied epileptogenic networks in each individual that can strongly distort the signal. Together, these limitations have has made group analysis of such data a statistically intractable problem. At present, only rudimentary approaches have been employed, and have included averaging across individuals in a common space in conjunction with statistical correction (82). Such an approach makes significant assumptions about intra- and inter-subject variability, fails to correct for the sparse sampling problem, and requires larges groups of subjects for a robust result (83, 84).

Overcoming these issues required a novel approach for the co-localization of ECoG data. We sought to first transform this data from a point source into a volumetric representation, and then apply fMRI group processing to the resultant datasets. Accounting for the different sources of variability and sparse data sampling required the use of mixed-effects, multilevel analysis (MEMA), an

approach recently developed for use with fMRI data (85). We studied a large cohort of individuals were who performed visually cued retrieval of common nouns and verbs (48, 76, 78, 86) during ECoG data acquisition. We then applied our new group analysis technique to these data to analyze the spatio-temporal distinctions of these different grammatical classes.

Methods

Data were collected from 19 patients (12 female, mean age 33 +/- 12 years) undergoing left hemispheric subdural electrode (SDE) implants for localizing seizures onset sites and from 14 healthy volunteers (Table 2.1). Informed consent was obtained following study approval by our institution's committee for protection of human subjects. Patients were selected to be able to perform the task within normal response parameters and possessed an average or higher IQ (Mean IQ - 98 +/- 11). A total of 1942 individual subdural electrodes were implanted. Of these, 313 electrodes were excluded due to proximity to sites of seizure onset (162), inter-ictal spikes (89), or 60Hz noise (62); the remaining 1629 SDEs were analyzed. There was excellent coverage over all canonical language cortex, including lateral frontal, lateral temporal and ventral occipito-temporal cortex (Figures 2.1 and 2.2). The extent of coverage allowed for meaningful grouped analysis of the temporal order in language processing. The methods involved in data acquisition and pre-processing are similar to those detailed previously (68, 87, 88).

Language tasks

All patients and healthy volunteers performed three language tasks (89) – naming of visually presented common nouns (Boston Naming Test), visual depictions of actions and scrambled images (generated from the noun and verb stimuli). Stimuli consisted of simple line drawings, akin to those found in Snodgrass and Vanderwart (90). During noun generation, subjects responded with single word descriptions of the object presented, and during verb naming, they responded with a single action word such as "*cooking*" or "*walking*". In response to the scrambled images, subjects articulated "*scrambled*", which provided us with a high-level control condition. During ECoG recordings, patients verbally articulated their response, while during fMRI acquisition both patients and healthy volunteers were asked to internally (covertly) vocalize and respond with a button press recorded by the stimulus presentation software (Figure 2.2).

From Conner et al Cerebral Cortex 2013

Pt Num	Sex	Age	Site	LI	Wada	CSM	Hand	IQ	Exp1	Exp2
1	F	37	L	0.56	L	L	R	89	x	x
2	M	21	L	0.40	L	L	R	97	x	x
3	M	39	L	0.52	n/a	L	R	100	x	x
4	F	38	L	0.27	L	L	R	96	x	x
5	M	17	L	0.43	L	L	L	67	x	x
6	F	30	L	0.56	L	L	R	107	x	x
7	F	20	L	0.72	n/a	L	R	103	x	x
8	F	30	L	0.82	L	L	R	100	x	x
9	F	20	L	0.28	n/a	L	R	97	x	x
10	F	42	L	0.80	L	L	R	107	x	x
11	F	28	L	0.77	L	L	R	97	x	x
12	F	51	L	0.19	L	L	R	92	x	x
13	M	42	L	1.00	L	L	R	109	x	x
14	M	23	L	0.89	L	L	R	91	x	x
15	F	29	L	0.46	L	n/a	R	83		x
16	F	45	L	n/a	L	L	R	93	x	x
17	F	21	L	n/a	L	L	R	78		x
18	M	30	R	0.44	L	n/a	R	90		x
19	M	27	R	0.78	n/a	Neg	R	112		x
20	M	40	R	0.84	n/a	n/a	R	94		x
21	F	51	R	0.91	L	n/a	R	74		x
22	F	28	R	0.30	n/a	n/a	L	107		x
23	F	62	B	0.33	L	n/a	R	93	x	x
24	M	56	B	0.79	n/a	Neg	R	116	x	x
25	M	24	B	n/a	L	n/a	R	105	x	x
26	F	30	B	0.24	L	n/a	R	120	x	x
27	F	31	B	n/a	n/a	L	R	124		x

Table 2.1 Summary of patient demographics
Demographics of the 27 patients enrolled in the study. In 17 subjects, the Site of grid implantation was the left (L) hemisphere, in 5 it was over the right (R), and in 5 SDEs were placed bilaterally. Laterality indices (LI) computed using fMRI of the same language tasks for 23 subjects. An LI > 0 indicates a left hemisphere dominant for language. In 13 subjects, intracarotid injection of sodium amytal (the Wada procedure) was also used to determine language laterality. Cortical stimulation mapping (CSM) was performed in 19 subjects, of which 17 were mapped over the left hemisphere and two over the right (patient no. 19 and 24). In all tested subjects, either deficient was produced on the left (L) or not seen on the right (Neg). Handedness was scored in all subjects using the Edinburgh Handedness Inventory (91), and revealed that 25 subjects were right hand dominant and 2 were left hand dominant. Not all subjects were included in both experiments, the presence of a subject in analysis is indicated in the Exp1 and Exp2 columns of the table.

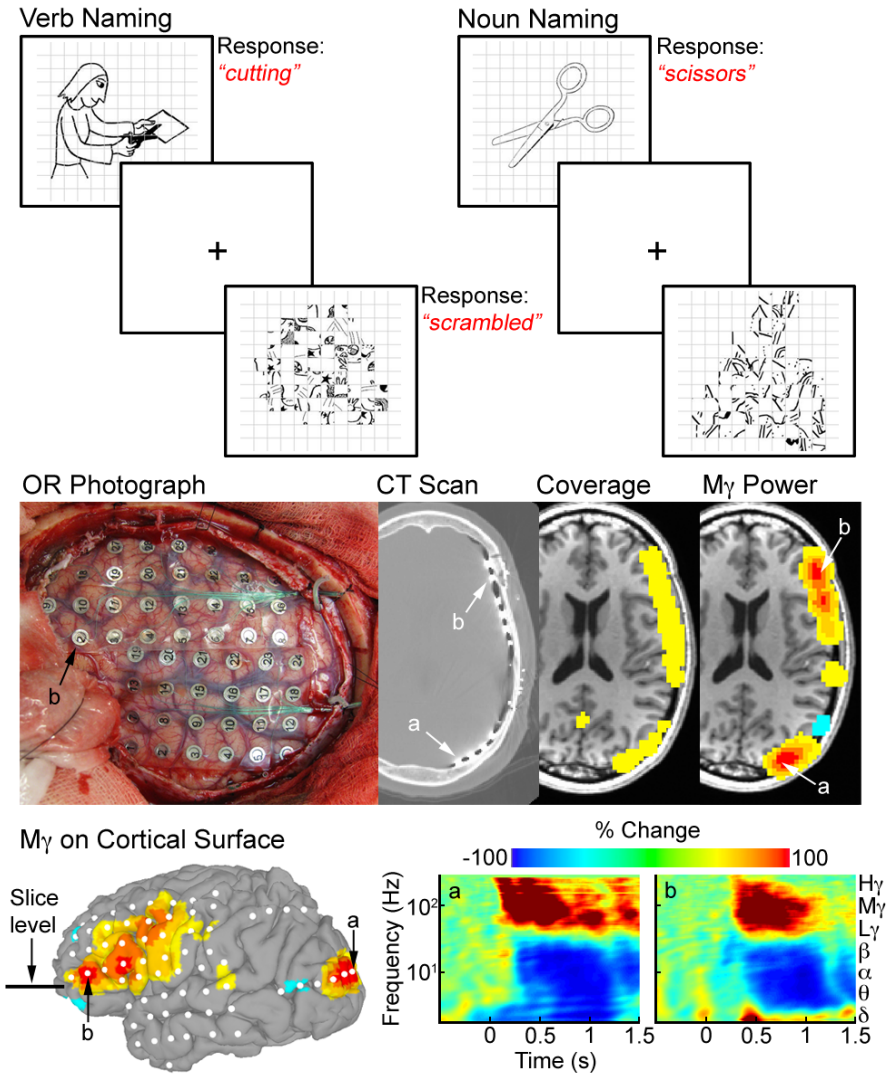

Figure 2.1 Task design and overview of analysis
Top Three language production tasks were used for both fMRI and ECoG: pictorially cued noun and verb generation, and naming of "scrambled" images. **Middle** Subdural electrodes (SDEs) were implanted after MRI acquisition and localized onto a cortical surface model. Two SDEs – (a) over the occipital pole and (b) over Broca's area, are shown at each stage of the processing at the slice level shown below. Volumetric representations of electrode distribution (or coverage) and of spectral changes (mid gamma power) in ECoG were made in imaging space. ECoG signal was calculated by filtering into the frequency band of interest and applying a Hilbert transform. Activity between stimulus onset and articulation was compared to baseline (-700 to -200ms). **Bottom** ECoG data represented on the cortical surface akin to fMRI analyses. Spectrograms for loci a and b following stimulus presentation show characteristic gamma band power increases and low frequency decreases. (Used with permission from Conner et al 2013 Cereb Cortex)

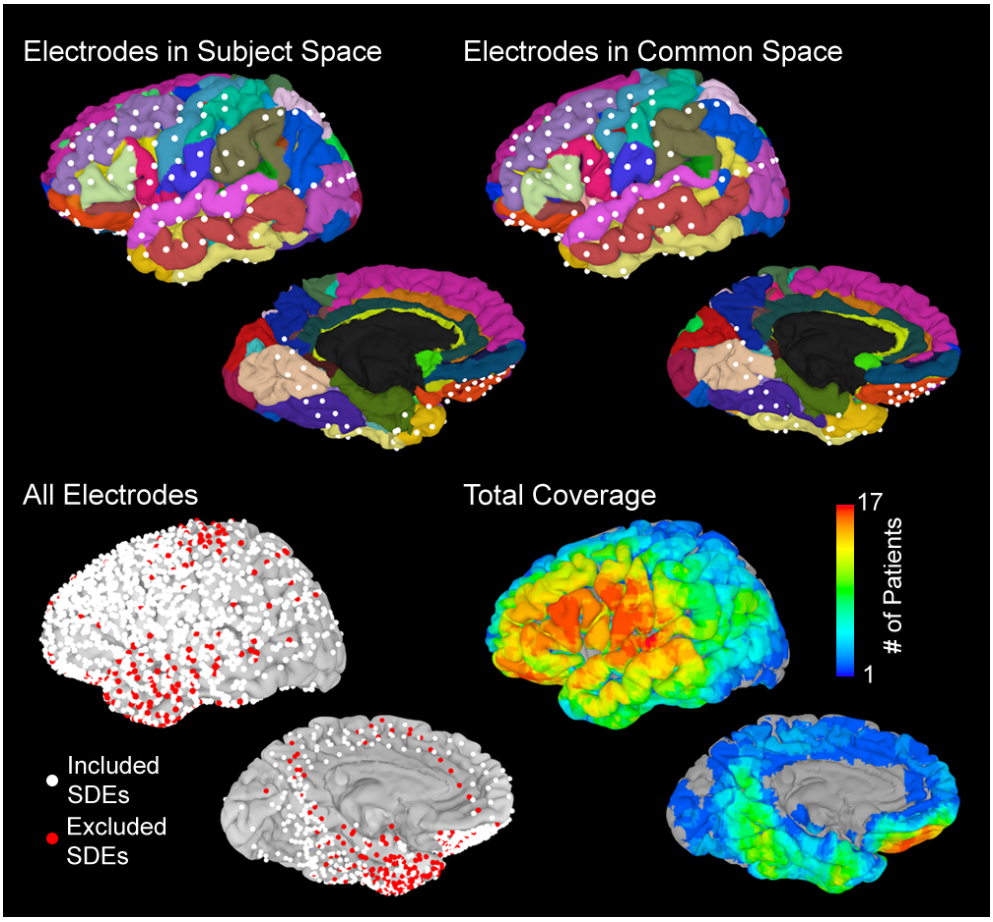

Figure 2.2 Distribution of electrodes used in the analysis
Top Left: SDEs localized in individual subject space and viewed on an automatically parcellated cortical surface. Right: Using a rigid, 12-parameter affine transformation, electrodes were aligned with the MNI-N27 brain in Talairach coordinate space. **Bottom** All electrodes for all subjects transformed into MNI-N27 space and displayed on the surface. SDEs over epileptogenic tissue or those with significant noise (red, n=313) were removed from the analysis. The remaining electrodes (white, n=1629) were used in the group analysis and to generate a total coverage map. (Used with permission from Conner et al 2013 Cereb Cortex)

MR Data Acquisition

Imaging data acquisition was performed with a 3T whole-body MR scanner (Philips Medical Systems, Bothell WA) equipped with a 16-channel SENSE head coil. The MR data were acquired prior to surgery. A magnetization-prepared 180^{o} radio-frequency pulses and rapid gradient-echo (MP-RAGE) sequence with 1mm thick sagittal slices and an in-plane resolution of 0.938 x 0.938mm and functional MRI volumes (thirty-three axial slices, 3 mm slice thickness, 2.75 in-plane resolution, 30 ms TE, 2015 ms TR, 90° flip angle) were collected. Language stimuli were presented in a block design (92). For each task (noun and verb generation), two runs of fMRI data were collected. Each run comprised of eight blocks (136 volumes per run), each block comprised of 10 task stimuli and 7 scrambled stimuli. 160 individual noun and verb, and 224 scrambled stimuli were presented. Each stimulus was presented at the onset of a TR using Presentation software (version 11, Neurobehavioral systems) and a screen positioned above the eyes (IFIS, Invivo, Gaineville, FL), for 1500ms with a 515ms inter-stimulus interval (Figure 2.1).

Image Analysis

MRI realignment, spatial normalization transformation and group analysis were performed in AFNI (93). Surface reconstructions of the pial surface were generated using FreeSurfer v4.5 (94). The aligned 4D dataset was spatially smoothed with a 3 mm Gaussian filter, then processed using multiple regression at each voxel to contrast the two tasks (noun and verb generation) with the control condition (scrambled naming). Both the effect estimates (regression coefficients) and their corresponding *t*-values were used for group MEMA analysis.

Laterality estimates

To verify left hemisphere language dominance, language lateralization indices were calculated for each individual using the language fMRI data (68). Activations in Brodmann areas 44 and 45 in each hemisphere were extracted using masks constructed from a standard atlas (53). The number of significant voxels ($p<0.001$) during the two tasks, verb and noun naming, were computed for the mask in each hemisphere. The laterality index used was equal to (#L - #R)/(#L + #R), were #L and #R are the number of significant voxels in the left and right hemispheres, respectively. In the 17 patients with fMRI data, all were left hemisphere lateralized for language function; of the 14 healthy volunteers, all were left hemisphere lateralized. Additionally, 12 patients underwent intra-carotid injection of sodium amytal (the Wada procedure) (95) and were found to be left-hemisphere dominant for language. Lastly, all but one underwent language localization using cortical stimulation mapping and were found to have eloquent language in the left hemisphere (96).

Electro-corticography

ECoG recordings were performed using arrays of subdural platinum-iridium electrodes (PMT Corporation, Chanhassen, MN) with a top hat design (4.5mm diameter, 3mm diameter contact with cortex) embedded in silastic sheets (10mm center-to-center spacing), using standard neurosurgical techniques (96, 97). SDEs were localized using post-op CT sans and in-house software, onto a cortical surface model (97). Stimulus presentation was carried out using identical stimuli and Presentation software as used for fMRI. In all patients, >50 trials of noun, verb and scramble naming were performed. Each image was displayed on a 15" LCD screen positioned at eye level for 1500ms with an inter-stimulus interval of >3000ms. A transistor-transistor logic pulse triggered by the Presentation software at stimulus onset was recorded as a separate input during the ECoG recording to time lock all trials. Audio recording of each ECoG session was used to accurately measure the onset of articulation and to compute reaction time. Only trials in which the patient responded correctly in <2s were included in further analysis. ECoG data were also visually inspected for inter-ictal epileptiform discharges and electrical noise. For 17 patients, ECoG data were collected at 1000Hz using NeuroFax software (Nihon Kohden, Tokyo, Japan. The other two patients underwent ECoG data collection at 2000Hz using the NeuroPort recording system (Blackrock Microsystems, Salt Lake City, UT). To avoid including any brain regions with potentially abnormal physiology, all electrodes that showed inter-ictal activity (spikes) or that were involved with seizure onset were excluded from all further analysis. All electrodes with greater than 10dB of noise in the 60Hz band were also excluded.

For the individual measures of activation during task performance, spectral analysis using the Hilbert transform and analytic amplitude were used to estimate power changes in different frequency bands. The raw ECoG data were band-pass filtered (IIR Elliptical Filter, 30dB sidelobe attenuation) into seven bands: delta (0-4 Hz), theta (4-8 Hz), alpha (8-12 Hz), beta (12-30 Hz), low gamma (30-60 Hz), mid gamma (60-120 Hz), and high gamma (120-240 Hz). A Hilbert transform was applied and the analytic amplitude was smoothed (Savitzky-Golay FIR, 2^{nd} order, frame length of 255 samples) to derive the time course of power in each band. The percent change and *t*-value at each time point were calculated by comparing power to the pre-stimulus baseline (-700 to -200ms). The epoch from 50ms after stimulus onset to mean RT minus 1 sd was selected for further analysis in order to minimize the effects of articulation on the ECoG. The composite *t*-value and effect size for this time-interval of ECoG data were then computed (metafor package ver 1.4 in R) (98).

Volumetric representation of ECoG Data

The time-integrated ECoG activity was transformed into volumetric data for each subject individually (68), to reflect the cortical regions that the recordings likely originated from. This transformation also enables grouped

analysis and minimizes errors in co-registration. The Euclidean distance from each electrode to each voxel in image space was computed and then this distance was scaled using 3D Gaussian filters (sd=6mm). This transformation was chosen because it maximizes agreement with fMRI results (68) and concurs with our limited understanding of ECoG signal sources (99). The net activity at each voxel was defined as the weighted sum of all SDEs that contributed to it. Individual volumes of activity were then constructed for noun, verb and scrambled naming. This transformation produced a 3D blur of the original, point estimate data provided by the SDEs. Additionally, an SDE coverage map was constructed for each individual subject - all voxels within 10mm (equal to the spacing between individual SDE electrodes) of an SDE were given a value 1, and all other voxels were set to 0. This binary map represents the volume of approximate SDE coverage for each subject and was then summed across all 19 individuals to obtain a total group coverage map (Figure 2.2), thresholded values of which were then used to constrain the group fMRI results. This is essential as the fMRI data are "whole brain", while the ECoG data, even for the large group used here, provide data for only parts of the cortex.

Spatial Normalization

For the grouped analysis, the datasets (both ECoG and fMRI) for each subject were aligned to the MNI-N27 brain. This alignment was performed by first computing the transform of the individual's anatomical MRI to the N27 anatomical MRI. The 12 parameter affine transformation of the individuals anatomical MRI was then applied to each individual's fMRI and volumetric ECoG data. In this manner, all of the ECoG datasets (n=19), the patient fMRI data (n=17), and the healthy volunteer fMRI data (n=14) were all transformed into the MNI-N27 imaging space.

Population level analysis of ECoG and fMRI data

Two methods were adopted in our group analysis of fMRI and ECoG data. The traditional approach for performing group analysis (e.g., *t*-test and two-way, mixed effects ANOVA) assumes that the effect estimates across subjects have the same reliability (or variance). In contrast, the MEMA approach takes both effect estimates (percent change for ECoG and regression coefficient for fMRI) and their variances for each individual to estimate of cross subject variability using restricted maximum likelihood function based on each subject's precision information of effect estimate (85).

Statistical Corrections

In order to correct for multiple comparisons, clustering analysis was applied to both fMRI and ECoG group analyses (to each ANOVA and MEMA test). An initial threshold of $p<0.05$ (uncorrected) was applied to select voxels of interest, and then grouped to get the number of contiguous voxels in each cluster. To determine the minimum size of a significant cluster, samples of white noise with the same dimensions and smoothness of the datasets were

generated. Only clusters greater than the minimum size (359 voxels) at the corrected $p<0.05$ were visualized.

Conjunction Analysis

To assess the difference between noun and verb naming, a conjunction analysis was applied to the verb vs. scramble and noun vs. scramble conditions (Figure 2.3). These maps were individually thresholded at $p<0.05$ (corrected), binarized and consolidated to identify regions of co-activation and areas only involved in one task (Figure 2.4). This comparison of verb vs. noun highlights regions that may not otherwise be considered significant (100).

Time Series Analysis

To estimate the average group time course for different regions, loci with the greatest divergence over the entire response epoch in activity between verb, noun and scrambled naming were identified from the 3D, volumetric group analysis (Figures 2.3 and 2.4). A total of twelve regions were used for this analysis. The coordinates at the center of mass for each region were then used to select SDEs from each individual that lay within 8mm of those co-ordinates (Table 2.2). For each region, percent change in the mid gamma band was averaged across the electrodes in that region from -500 to 2000ms for each of the three tasks (Figures 2.5 and 2.6).

Comparison of Group fMRI vs. Group ECoG

The results of grouped fMRI and ECoG datasets were compared with a voxel-based approach derived using the beta coefficients from the MEMA. Both sets of beta coefficients (7 values in the ECoG dataset, one corresponding to each spectral band; and a single value for the fMRI), along with the ECoG coverage map, were utilized. Correlations were made only for voxels with a >5 patients contributing to the ECoG (see coverage map – Figure 2.2), and were rerun for voxels with increasing coverage (greater numbers of patients contributing to the data) to a maximum of 15 to model goodness of fit. In order to evaluate the effect of fMRI group size and correlation with ECoG, a bootstrapping analysis was run using the individual fMRI datasets. The group of 17 subjects with both fMRI and ECoG data were resampled with replacement (500 resamples) for different fMRI group sizes (3, 5, 7, 9, 11, 13, and 15) and then each new group was re-analyzed with MEMA. The resulting beta coefficient maps for each resample were correlated with the ECoG group results (using all 19 subjects). Only voxels that were sampled in ECoG for at least 10 patients were used to ensure for an adequate number of subjects. The distribution of resamples was used to model the correlation of fMRI to ECoG at the different group sizes. Differences between group sizes distributions were performed using sign tests (Bonferroni corrected $p<0.001$).

From Conner et al Cerebral Cortex 2013

Results

Behavioral results

Behavioral responses were collected for all patients (n=19) during ECoG recordings and most patients during fMRI acquisition. During ECoG, the mean reaction times (RTs) were 1377ms (sd = 274ms) for noun naming, 1479ms (sd = 262ms) for verb naming, and 1210ms (sd = 285ms) for scrambled images. RTs for verb and noun naming were significantly longer than for the scrambled controls (paired t-test, $p < 0.01$). As expected, verb naming had a significantly longer RT than noun naming ($p = 0.03$) (101). Mean accuracy for all tasks was >90%, although only correct naming trials were included in the analysis. During fMRI, the mean RTs were 952ms (sd = 115ms) for noun naming, 1082ms (sd = 225ms) for verb naming, and 736ms (sd = 178ms) for scrambled images. As in the ECoG, verb and noun naming were both significantly longer than scrambled naming ($p < 0.01$), and the latency of verbs was also greater than nouns ($p = 0.03$). To verify that this difference was not due to word frequency, the frequency of verb and noun stimuli (using the SUBLEX word frequency database) were compared and found not to be significantly different (Wilcoxon rank sum, $p = 0.2$) (102). Given that response time during MRI acquisition was measured using a button press, the difference between the two recording modalities likely reflects the delay due to voice onset time in ECoG and the button press instead of overt articulation in the fMRI condition.

Grouped ECoG analysis

MEMA of visual naming of both nouns and verbs compared with scrambled picture naming (epoch from stimulus onset to just before articulation was considered a single block) revealed strong, high-frequency power increases for both categories over the inferior frontal gyrus (IFG), basal temporal, precuneate, pre-motor and M1 cortices (Figures 2.3 and 2.4). Categorical distinctions (corrected $p<0.05$) were obvious in the posterior para-hippocampal gyrus (PHG), which was more active during noun generation, while pars orbitalis of the IFG, inferior parietal lobule, and superior lateral occipital cortex (SLOC) were significantly more active during verb generation (Figure 2.4 and Table 2.2). Cortical regions were always more active (in the gamma band - 30-240 Hz) during naming of real nouns or verbs relative to the scrambled images except for the anterior superior frontal sulcus.

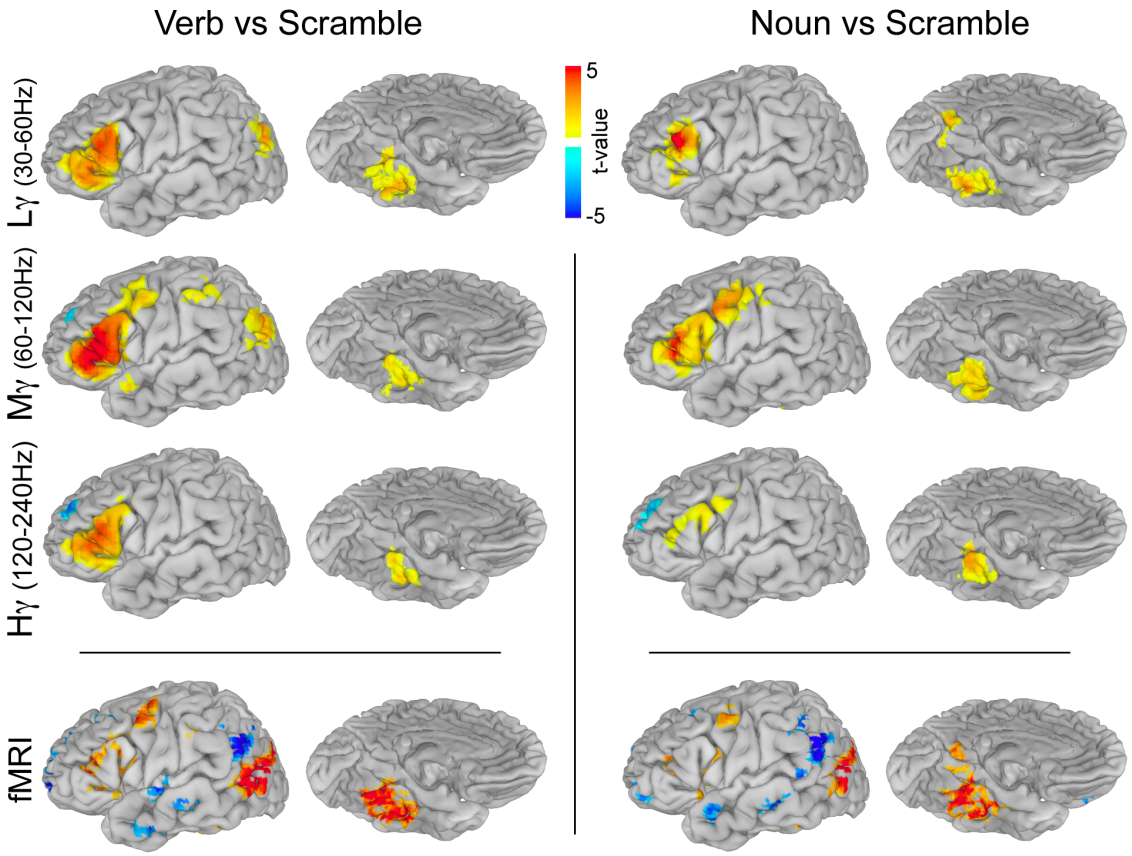

Figure 2.3 Verb and noun naming contrasted with scrambled images
ECoG (n=19) group analysis was carried out using mixed effects, multilevel analysis for low gamma (30-60Hz), mid gamma (60-120Hz) and high gamma (120-240Hz) (corrected $p<0.05$). The time window used was from 50ms after stimulus presentation until 1 sd before mean articulation. The fMRI (n=17) group analysis was performed using an ANOVA (corrected $p<0.05$), and only regions with a minimal SDE coverage of $n\geq5$ (Figure 2.2) are depicted. (Used with permission from Conner et al 2013 Cereb Cortex)

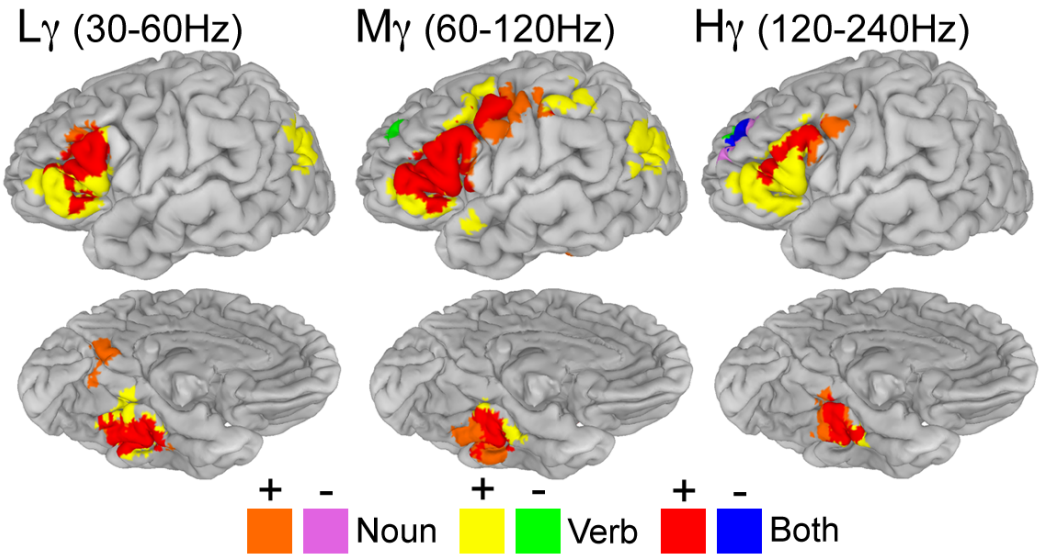

Figure 2.4 Group verb minus noun naming and conjunction analysis
Conjunction analysis of verb vs. scrambled and noun vs. scrambled results (n=19) thresholded at a corrected p<0.05 (Figure 2.3) and visualized to identify regions active during either one or both tasks. (Used with permission from Conner et al 2013 Cereb Cortex)

Grouped ECoG time series analysis

The time series of all electrodes across all individuals, located in cortical regions with significant differences in the MEMA results, revealed prominent early activity (100-200ms) in the ventral occipito-temporal region – the posterior inferior temporal gyrus, the fusiform gyrus and the posterior PHG (Figures 2.5 and 2.6). Activity in these areas continued to be significantly elevated from baseline well past the onset of articulation. Early activity was also was noted in Broca's area, lateral premotor cortex and in M1 mouth beginning around 300ms, peaking at 700ms, and lasting till past the onset of articulation. These timelines imply non-hierarchical interactions between these regions, contradicting previously proposed models of serial order in language processing (103). To confirm that the patterns of activity in the group analysis reflected individual data well, single subject time series analyses were also performed (Figure 2.5). These single electrodes were chosen to overlap with the regions used in the grouped analysis and corroborate those findings.

From Conner et al Cerebral Cortex 2013

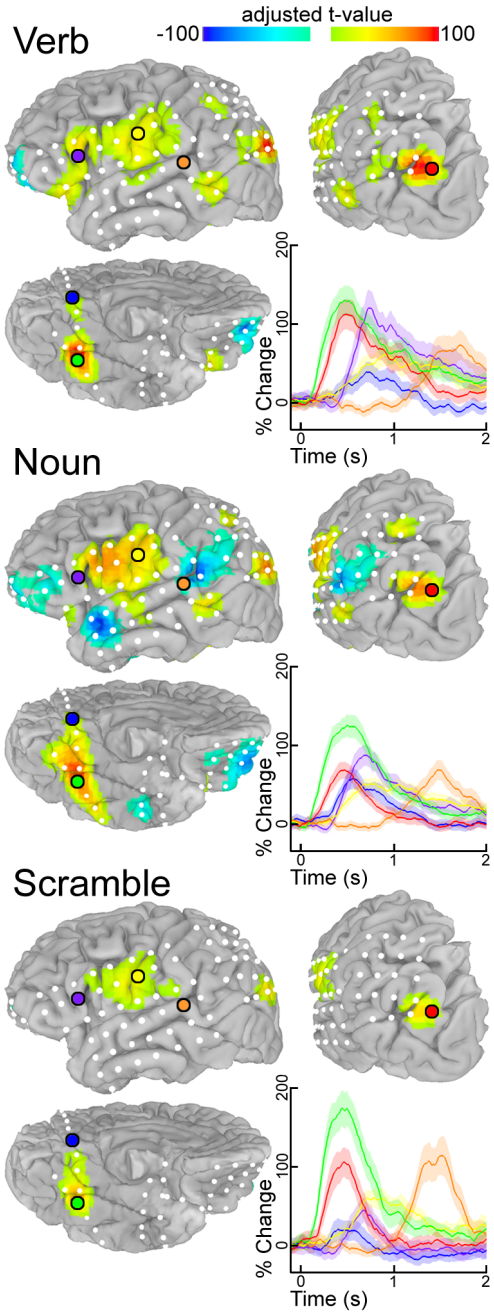

Figure 2.5 Single subject ECoG analysis
Both the time integrated (mid gamma - 60-120Hz frequency range, 50ms after stimulus presentation to 1 sd before mean articulation) and the time series analysis results are depicted for a single subject (time locked to stimulus presentation). Location and percent change (relative to pre-stimulus baseline) are shown for six representative electrodes over pars triangularis (purple), primary motor (yellow), STG (orange), SLOC (red), posterior PHG (blue), and fusiform gyrus (green) during each of the three tasks. (Used with permission and modified from Conner et al 2013 Cereb Cortex)

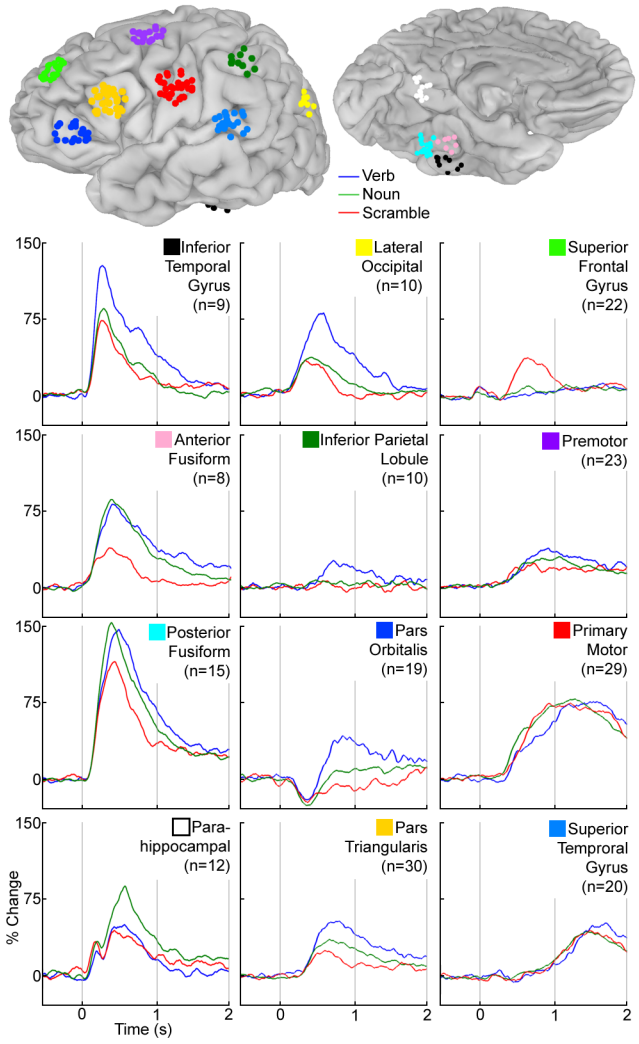

Figure 2.6 Average time series for regions with significant activation
SDEs within 8mm of center of mass of significant activations for verb vs. scramble or noun vs. scramble using 3D MEMA (Figure 2.3) were selected. The percent change in the mid gamma band (60-120Hz) over pre-stimulus baseline was calculated and averaged for these electrodes in these 12 regions. The location of all electrodes in these regions is shown on the MNI-N27 brain surface (co-ordinates in Table 2.2). (Used with permission from Conner et al 2013 Cereb Cortex)

Additionally, when ventral occipito-temporal electrodes were closely analyzed, a medio-lateral gradient favoring noun-to-verb naming was noted, with nouns production resulting in the greatest activation overall, but especially so over the posterior PHG where a late response (500ms) was greatest for nouns relative to verb and scramble conditions. This response followed an earlier peak corresponding to the N100 response over primary visual cortex. The SLOC also showed strong, early (300ms) activation, greater and more sustained during verb naming than during noun and scramble conditions, in keeping with the MEMA results. Activity in motor cortex and in superior temporal gyrus (STG, primary auditory cortex) was vastly similar across conditions, implying minimal differences in articulatory difficulty or length between these conditions.

An intriguing response was noted in pars orbitalis, where all of the naming tasks produced an initial net decrease in gamma power followed by a significant increase during verb generation. The time series analysis also clearly demonstrated that the superior frontal sulcus deactivations noted for both verb vs. scrambled and noun vs. scrambled contrasts are not due to a decrease in power during the task condition, but rather due to an absolute power increase during the scrambled condition starting at 400ms and peaking at 600ms.

Grouped fMRI analysis

fMRI analysis of the nouns and verb production elicited broadly similar patterns of activation as revealed by the MEMA of the ECoG data (Figure 2.3). Again, verb generation led to greater amplitude and spatial distribution of activation overall. For both lexical categories, clear increases in activity were noted in the ventral occipito-temporal cortex, specifically centered in anterior fusiform gyrus - as revealed in many other prior studies (104, 105), the lateral temporo-occipital junction (79), Broca's area and M1 mouth. Significantly, no increase in activity in the lateral temporal neocortex was noted during either of these naming tasks, in agreement with prior studies (106). A strong focus of deactivation was noted at the temporo-parieto-occipital junction, corresponding to greater activity in the control than the task condition. Lastly, a small but consistent focus of deactivation in the SFG was noted for both tasks relative to scrambled naming, similar to that seen during ECoG.

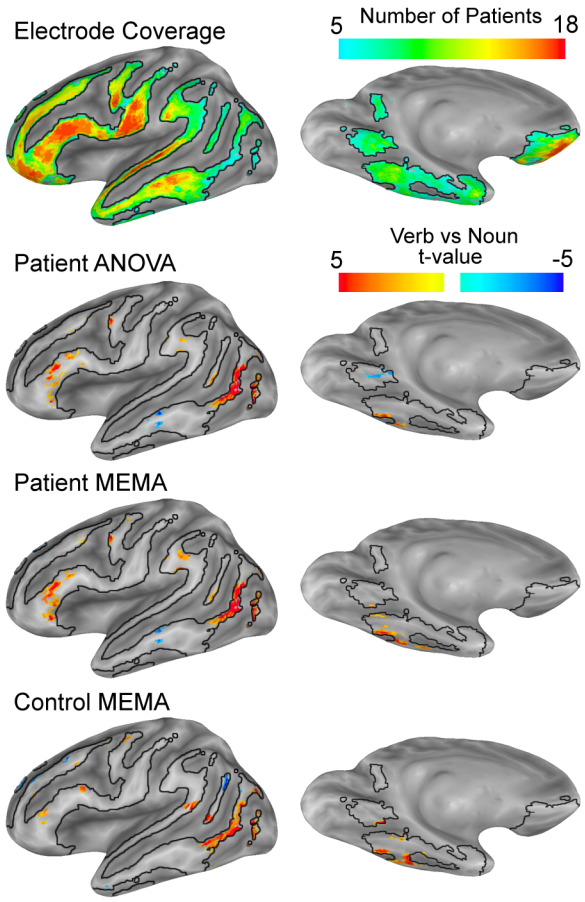

Figure 2.7 Grouped analysis of fMRI data
All data were constrained by the electrode coverage map (n≥5). Patient data (n=17) were processed using an ANOVA and a mixed effects, multilevel analysis (MEMA) to determine differences between verb and noun generation. MEMA and ANOVA analyses show vastly similar results. fMRI data from healthy subjects (n=14) doing the same task, and processed the same way shows no salient distinctions compared with the patients, confirming the validity of this analysis to the study of “normal” language. (Used with permission from Conner et al 2013 Cereb Cortex)

MEMA comparing verb and noun generation of the fMRI data performed on both the patient and the healthy controls revealed vastly similar results (Figure 2.7). There was greater activation for verbs than nouns in pars orbitalis, anterior pars triangularis, M1 mouth and lateral temporo-occipital cortex. The PHG was more active for noun rather than verb generation, while the ITG was more active in verb generation, recapitulating the lateral to medial bias of verbs to nouns seen with ECoG. While the middle temporal gyrus appeared to be more active in noun rather than verb generation, it was not active in either one of these conditions when compared with baseline (86).

From Conner et al Cerebral Cortex 2013

ECoG		
Inferior Temporal	-43, -39, -26	BA36
Fusiform	-29, -43, -19	BA20
Parahippocampal	-6, -53, 0	BA18
Precuneus	-1, -57, 16	BA23
Lateral Occipital (SLOC)	-43, -75, 26	BA39
Supramarginal	-60, -47, 23	BA40
Superior Temporal	-64, -35, 14	BA22
Superior Frontal	-34, 46, 32	BA9
Pars Orbitalis	-54, 34, 3	BA45/47
Pars Triangularis	-56, 19, 19	BA45
Premotor	-41, 3, 52	BA6
Primary Motor	-61, -9, 28	BA4
fMRI		
SFG (deactivation)	-27, 34, 40	BA8/9
Lateral temporo-occipital	-53, -65, 1	BA37/19
IFG (pars orbitalis)	-47, 27, 4	BA45/47
IFG (pars triangularis)	-48, 25, 16	BA45
Premotor	-44, 2, 44	BA6
Superior Occipital Gyrus	-38, -75, 28	BA19
Fusiform	-38, -45, -15	BA37

Table 2.2 Spatial coordinates of peak activation sites
Regions with ≥5 subjects and a significant ($p<0.05$, correct with cluster analysis) activity were localized in Figures 2.3, 2.4, and 2.7. These regions were used to seed the group ECoG time series analysis (Figures 2.5 and 2.6). Co-ordinates are shown in Talairach space. (Used with permission and modified from Conner et al 2013 Cereb Cortex)

Limitations

While this analysis does demonstrate the first application of a robust group analytic technique for ECoG datasets, there are some notable issues. The data from each subject are initially integrated over a long time epoch. This helps to standardize the window used for analysis across subjects. Given that each subject does not have the same reaction time, it stands to reason that there is some variability between subjects in how long each processing step requires. This can cause brief events to decrease in relative magnitude if the time epoch is too long. Overcoming this issue motivated the additional analysis using the grouped time series plots for the regions of interest. Another issue lies with the volumetric transformation of the data. We have chosen to transform the data using a 3-dimensional Gaussian function, and while we believe this to be the most reasonable option, several other functions (sphere/boxcar, exponential or linear decay) could have also been used. Given the current state of understanding about intracranial current decay (99, 107), more work is need to understand current spread for the purposes of ECoG source modeling. Further, this volumetric transformation was followed by an affine transformation to a common co-ordinate space. This is a method commonly applied to fMRI data sets, however, recent advances allow for more accurate registration techniques (108, 109). These algorithms respect sulcal and gyral anatomy, meaning that they are more suited for data that are cortico-centric, as ECoG are.

Conclusions

To resolve the debate over localization of different grammatical classes, we studied a large cohort of subjects using intracranial electrode recordings. In order to analyze these data as a single group, we applied a novel, statistically rigorous method of group ECoG processing. We found that both the spatial location and extent of activations varied in several regions based on the category of stimulus being named (noun, verb, or scrambled). In ventral temporo-occipital cortex, early PHG gamma activity (from 400-500ms) was greatest during noun generation and least during scrambled naming. Over lateral cortex, SLOC processing during verb naming was greatest in this same time window. These differences were reflective of a broader pattern of greater noun processing in the ventral stream, and greater verb processing in the dorsal stream; and were consistent with previous descripts of the roles of PHG in visually cued naming (104), and of the SLOC during action perception (79, 110) and action decoding (111). As a whole, these results strongly support the dual stream hypothesis of semantic processing that dissociates dorsal stream activity in verb generation (48), and a ventral stream activity in noun recall (112).

In prefrontal cortex, significant gamma power changes were seen in the ventro-lateral prefrontal cortex (VLPFC, BA45/47) during verb naming (500-1000ms) alone. This activation could be reflective of involvement of this region in action perception (111) and in syllabification (103). Furthermore, prior fMRI and MEG studies contrasting noun and verb production have found that VLPFC and premotor cortex were significantly more active during verb than noun generation

similar visual stimuli (75, 76, 78) and even auditory cues (113). In order to characterize the function of this activation, it will be necessary to determine if this region is functionally connected to the dorsal stream during verb naming and determine if this increased processing is due to semantics or phonology.

A significant activation of scrambled naming relative to both noun and verb generation over dorso-lateral prefrontal cortex (DLPFC) in both the ECoG and fMRI results. This was the only region were scrambled naming caused a greater response than either of the two other tasks. When this region was examined using the grouped time series analysis, we found that only scrambled naming caused any increase in gamma power for this region. When compared with activity in other regions, we found that the onset of this activity overlapped with activity in the SLOC and PHG during the lexical access portion of task performance. This is suggestive of an early identification of the scrambled image followed by rule access (articulate “scrambled”). Prior work has shown that the DLPFC is integral to task switching, cognitive control, monitoring of behavior (114, 115) and higher-level working memory (116), and several of these processes are likely in operation here.

In posterior left IFG, activation was not significantly different between noun and verb generation. We found that onset and duration of activity in premotor and primary motor (M1) cortices was similar across conditions, implying that the demand upon these regions was roughly equal during execution and monitoring of the articulatory plan (117). Importantly, activity in M1 and SLOC followed two different time courses, with SLOC being active during early stimulus processing and M1 being recruited much later. This suggests that these regions are engaged in a

fundamentally different process, in contradiction to the motor theory of language (30). One explanation is that motor semantics are largely stored in parietal cortex, while premotor and motor cortex are involved in direct planning and control of motor output. During all tasks, an auditory response was present in STG that was roughly equal in onset and magnitude. Given that the visual, motor and auditory responses were not significantly different between tasks, this suggests that the processing streams for these three language processes start and end at similar locations, but have divergent, intermediary paths.

A second goal of this study was to leverage the high temporal resolution of ECoG data for precise timing of cortical processing. Using grouped time series analysis, we investigated the temporal structure of word production to determine the degree of serial processing that was present. While this approach does not unambiguously reject a discrete processing architecture, this work definitively shows that the processing scheme is not comprised of modular, serial processes (15). Rather, distributed areas are active concurrently, implying parallel, non-hierarchical network processing.

CHAPTER 3: INFORMATION FLOW WITHIN BROCA'S AREA

Introduction

Given the historical significance of Broca's area in language processing and the level of activity found during noun and verb naming, we decided to examine the activity and network dynamics of this region in the context several different theories on LIFG function. In our second major goal, we sought to find the regions involved in response selection and controlled retrieval. Our hypothesis was that these two processes were not separate operations, but rather that controlled retrieval is an emergent property of the functional connectivity between LIFG sub-regions (58). Further, we predicted that the functional organization of this region would not exhibit a rostro-caudal hierarchy, and that processing here would proceed in parallel with reciprocal feedback.

The importance of information flow in these objectives required a robust method for estimating functional connectivity. From our previous work, the focus of this analysis was on higher frequency bands (gamma, >30Hz) (1, 68). In these frequency ranges, using spectral coherence is problematic because of the contribution of phase to this measure (118). Gamma oscillations do not frequently couple in phase over distances in cortex, greatly reducing the magnitude of the coherence above the beta band. Furthermore, use of Granger causality would also not be feasible because electrodes in each sub-region are frequently adjacent to one another and may therefore have common noise inputs or low frequency components that are hard to account for (119). An alternative to both of these measures are amplitude envelope correlations (AEC), a method that overcomes these issues at the expense of narrowing the frequency band of interest from the

onset (120) (see Appendix). AEC also allows for rapid calculation of time-lagged correlations, an imperative for studying interactions over long time windows.

Using the AEC method in conjunction with gamma power activation, we sought to validate several models describing the functions of LIFG sub-regions. Notably, we investigated the two-process theory, domain general and domain specific models of phonologic processing, and the selective involvement of motor cortex in the processing of verbs. Resolution of these issues is not possible in the absence of data with spatio-temporal resolution adequate to derive information about the dynamics within this region (63). In a large cohort of individuals implanted with subdural electrodes over the IFG in both hemispheres, we used measures of intra- and inter-areal dynamics to study semantics, retrieval and phonologic processes intrinsic to the naming of objects and actions.

Methods

Data were collected from 27 patients (17 female, mean age 33 +/- 12 years) undergoing left hemispheric subdural electrode (SDE) implants for localizing seizures onset sites (Table 2.1 and Figure 3.1). Informed consent was obtained following study approval by our institution's committee for protection of human subjects. All patients were able to perform the task within normal response parameters (Figure 3.2) and possessed an average or higher IQ (Mean IQ - 98 +/- 11). Of these 27 patients, 12 underwent intracarotid injection of sodium amytal (the Wada procedure) (121) for lateralization of language function and all were found to be left-hemisphere dominant. 24 of these patients also underwent language mapping using fMRI techniques and were all found to be left hemisphere dominant. 19 underwent language localization using cortical stimulation mapping that resulted in language production deficits in 17.

Functional Connectivity

Functional connectivity was assessed using amplitude envelope correlations (AEC) (122-124). Raw data were band pass filtered in the frequency domain between 70-110Hz using square filter with sigmoid flanks (half amplitude roll off of 1.5Hz) and Hilbert transformed. An inverse Fourier transform was applied, and the absolute value was taken and smoothed with a moving average (100ms long) to obtain the amplitude envelope of the signal. A noise correlation between pairs of channels was computed with the Pearson's correlation at each time point across trials. In order to estimate directionality of connectivity, the time series on one channel was lagged prior to AEC (120). For individuals, significance was estimated using boostrapping (trial re-shuffling, 1000 resamples using Matlab Parallel Computing Toolbox ver 6.1).

Grouped Functional Connectivity

In each individual, the SDEs localized in each area (POr, PT, POp, M1) were used to build a list of possible pairs between any two sub-regions. Given that each patient may have multiple SDEs in an area, it was necessary to limit the number of pairs from each person contributing to the group average. To do this, SDEs were only considered eligible if they met relatively low activation requirements. For left PT, POp, and M1, a 15% increase in gamma power relative to baseline was considered 'active', whereas in left POr SDEs were included if there was a 10% decrease. These criteria reduced the number of SDEs in each region to: 22 POr sites, 22 PT sites, 19 POp sites, and 28 M1 sites. The individual AEC results were computed for all SDEs in each individual, then transformed into a Fisher's z, averaged and assigned significance. For connectivity between each sub-regionthere were: 28 POr/PT pairs, 23 POr/POp pairs, 31 POr/M1 pairs, 29 PT/POp pairs, 39 PT/M1 pairs, and 41 POp/M1 pairs.

As activation in the right hemisphere was less, the inclusion criteria for right PT, POp, and M1 was a 10% increase in gamma power relative to baseline and in rigth POr it was a 10% decrease. These criteria reduced the number of SDEs in each region to: 7 POr sites, 12 PT sites, 8 POp sites, and 13 M1 sites. The numbers of pairs assessed were 6 POr/PT pairs, 4 POr/POp pairs, 9 POr/M1 pairs, 17 PT/POp pairs, 23 PT/M1 pairs, and 15 POp/M1 pairs.

Attractor State Dynamics

Attractor state dynamics were modeled using k-means clustering of the information flow between all regions (125). Time-series of connectivity were imported into R (ver 2.15.2, R Foundation for Statistical Computing) and grouped temporally. For the four sub-regions, six different pairs were possible (POr/PT, POr/POp, POr/M1, PT/POp, PT/M1, POp/M1), and connectivity for three different lags were considered (-0.2s, 0s, and 0.2s) to incorporate information flow in each direction. In this way, a total of 18 AEC time courses were used for clustering. Convergence and cluster order was validated using silhoutette plots (noun naming: 5 clusters, verb naming: 6, scrambled naming: 4) (126). Finally, clusters were visualized in phase space using principal components.

From Conner et al 2013 *in review*

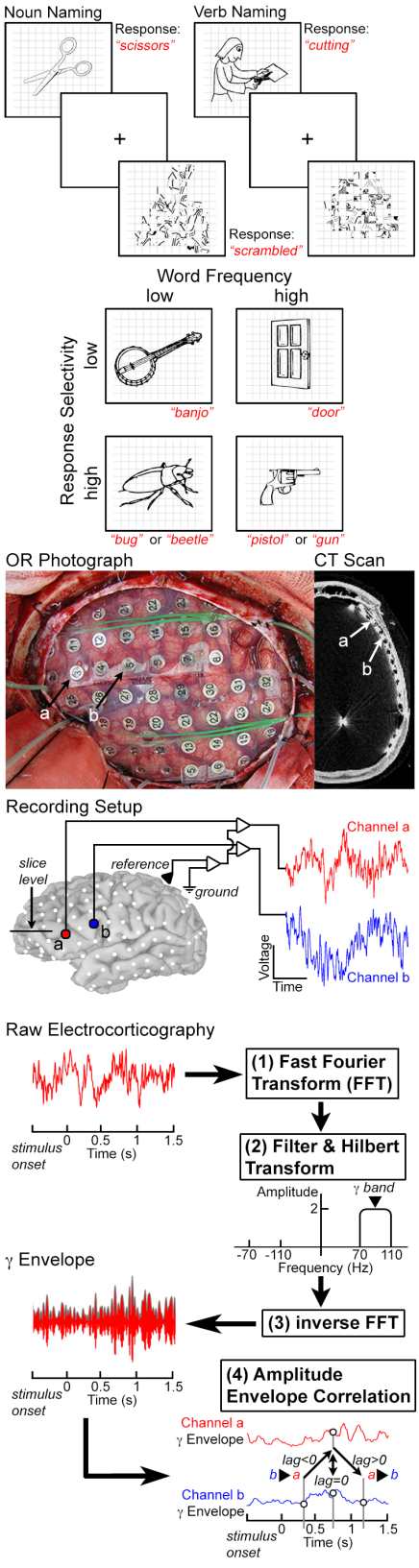

Figure 3.1 Task design and methods overview
Patients performed three visual naming tasks: verb, noun and scrambled naming, during which they responded by articulating a single word. Noun stimuli were classified based on word frequency and selectivity for further analysis. Electrocorticographic (ECoG) data were recorded from grids of sub-dural electrodes (SDEs) that were localized using CT scans. Data were recorded at 1-2kHz during task performance, and ECoG data were stored for offline analysis. To compute spectral power changes, data were fast Fourier transformed (FFT), then filtered and Hilbert transformed in the frequency domain prior to inverse FFT. The smoothed power envelope was then used for functional connectivity analysis using amplitude envelope correlations (AEC). By lagging the time series of one channel, directionality of information flow was estimated. Gamma band (70-110Hz) activity was used for power analysis and funcitonal connectivity (from Conner et al 2013 *in review*).

Results

Electro-corticographic (ECoG) data were collected in 27 left hemisphere language dominant patients implanted with 3351 SDEs during pictorially cued naming of nouns, verbs, and scrambled images (Figure 3.1) (1). Seventeen patients were implanted over the left hemisphere, five over the right hemisphere, and five bilaterally (68, 90) (Table 2.1). Noun stimuli were ranked based on lexical frequency (102), and selectivity (number of possible correct responses) (90). As expected, reaction times during the experiment were significantly longer for low frequency and high selectivity nouns ($p<0.001$, paired t-test) (Figure 3.2) (101).

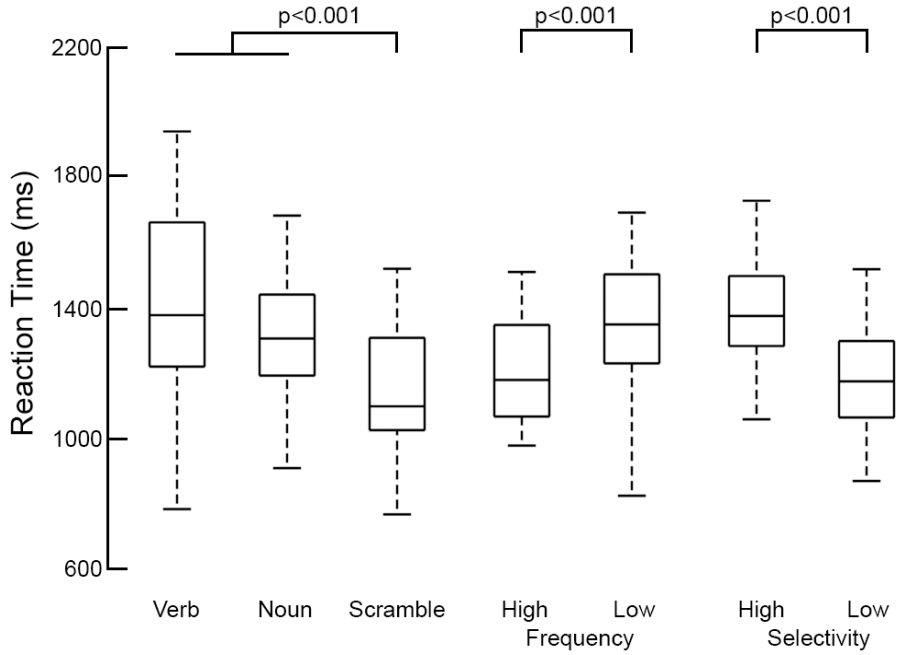

Figure 3.2 Reaction times for each condition
Both verb and noun naming had significantly higher latency than scrambled naming ($p<0.001$, two-sided, paired t-test), but were not significantly different from each other ($p=0.10$). High frequency words had a significantly shorter latency than low frequency words ($p<0.001$) (102), and high selectivity words had higher latency than low selectivity words ($p<0.001$) (90) (from Conner et al 2013 *in review*).

Following localization onto individualized automatically parcellated cortical surfaces, SDEs overlying LIFG and motor cortex were anatomically labeled as POr, PT, POp, or M1 sites. Time-frequency analysis was performed for all electrodes and averaged within each of these four sub-regions (Figures 3.3 and 3.4) (127). Activity in each region was quantified using power changes in the gamma frequency range (70-110Hz). Functional connectivity was assessed using amplitude envelope correlations (AEC) of power fluctuations in the gamma range and the directionality of connectivity was determined by lagging the time series of one channel (120, 122, 123).

> At the level of each individual and across the group, the first notable change was a dramatic decrease in gamma power in POr below baseline. This began 250ms after stimulus onset and preceded the concurrent activation seen in PT, POp and M1 by 150ms. Task related distinctions were noted in POr and PT and included greater activity during verb > noun > scrambled ($p<0.01$, two-sided paired t-test, FDR corrected). Activity in POp and M1 was similar across conditions, but articulation of verbs occurred with longer latency and duration (Figures 3.3 and 3.4). High selectivity nouns preferentially engaged PT more than those with smaller numbers of possible responses starting at 600ms after stimulus onset ($p<0.01$, FDR corrected) (Figure 3.3). However, lexical frequency was not associated with distinctions in activity in any sub-region (Figure 3.5). In the right hemisphere, an identical analysis revealed that only M1 was significantly active (Figure 3.6).

From Conner et al 2013 *in review*

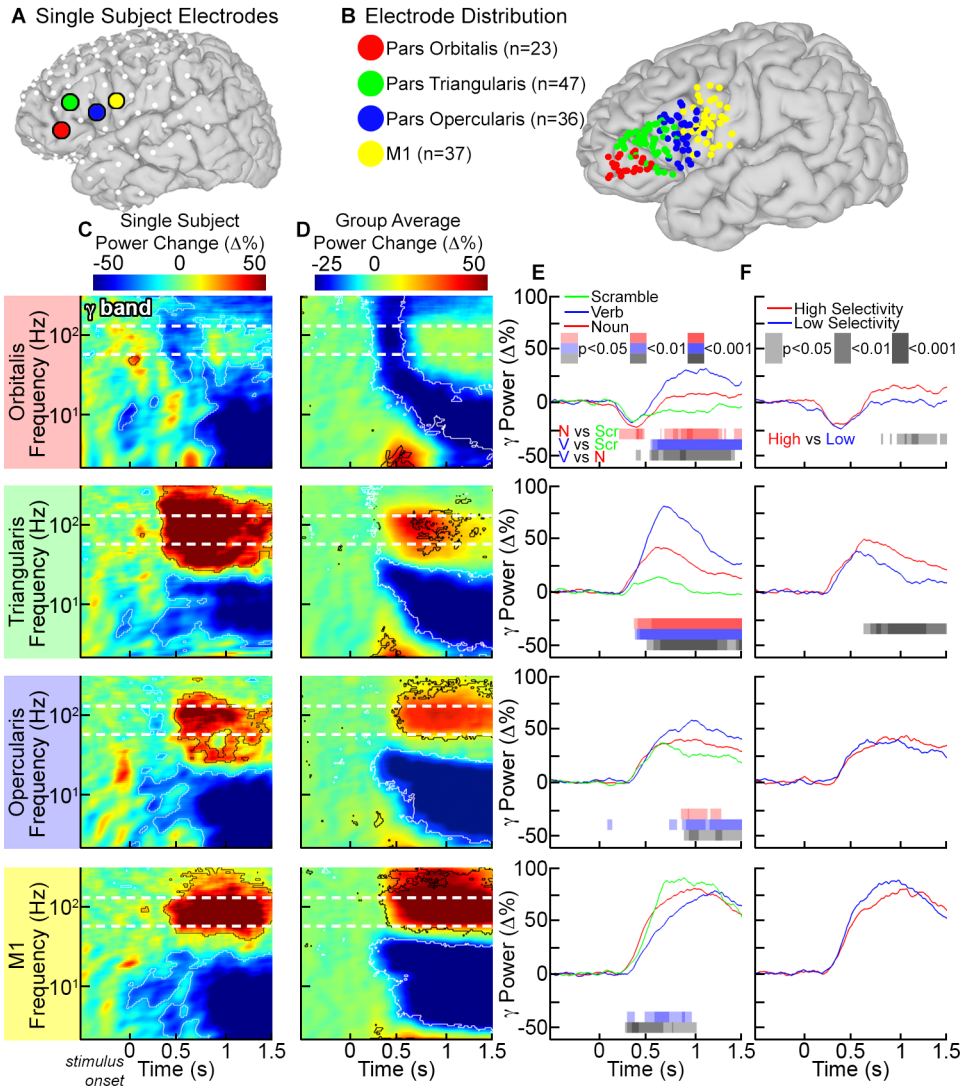

Figure 3.3 Time-frequency analysis of noun naming
(**A**) SDEs from each individual were anatomically localized POr, PT, POp, and M1. (**B**) SDEs from the 22 subjects with left hemisphere implants were co-localized on a common brain surface. (**C**) Single and (**D**) grouped time frequency reponses during noun naming (percent power change relative to pre-stimulus baseline, p<0.01 FDR corrected, t-test for single subject, two-sided sign test for group). Gamma (70-110Hz) power changes were compared in the group for (**E**) all three tasks and (**F**) high or low selectivity nouns across subjects (paired t-test, two-sided, FDR corrected) (from Conner et al 2013 *in review*).

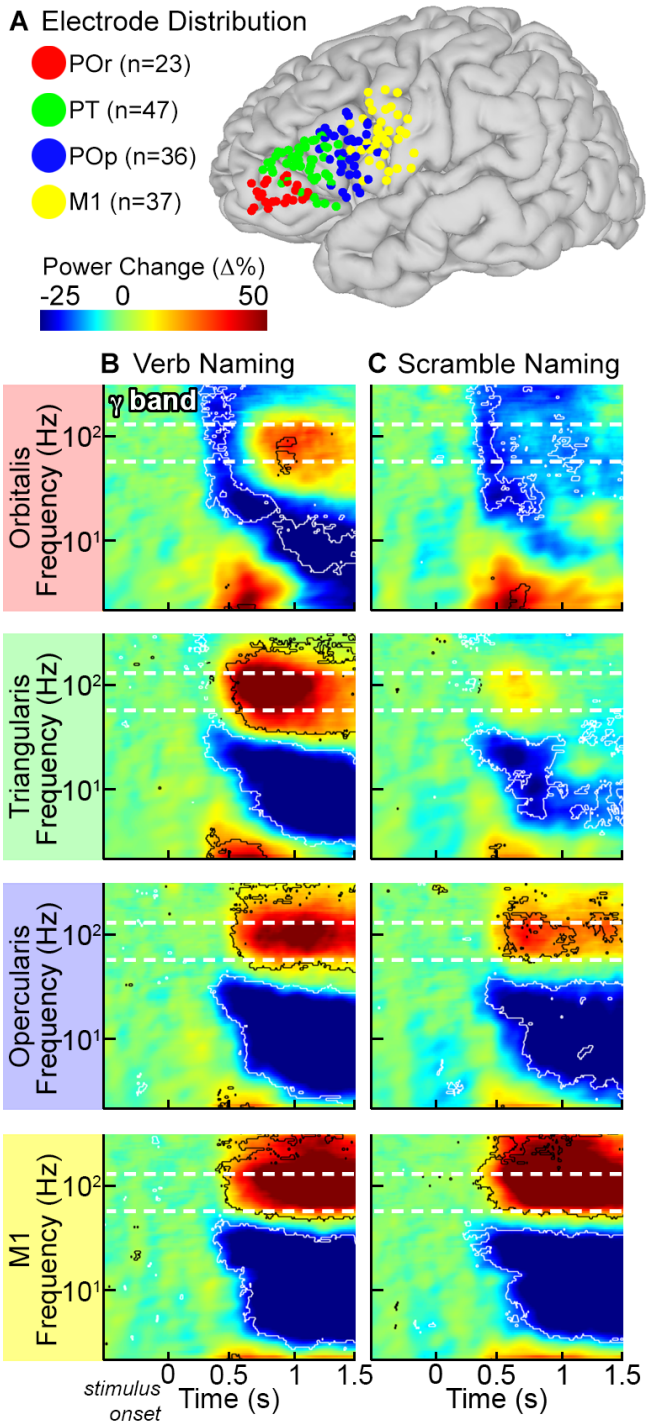

Figure 3.4 Time-frequency results of verb and scramble naming
Group analysis of (**B**) verb and (**C**) scrambled naming using the same method as applied to noun images (Figure 3.3, p<0.01, two-sided sign test, FDR corrected), normalized to pre-stimulus baseline (from Conner et al 2013 *in review*).

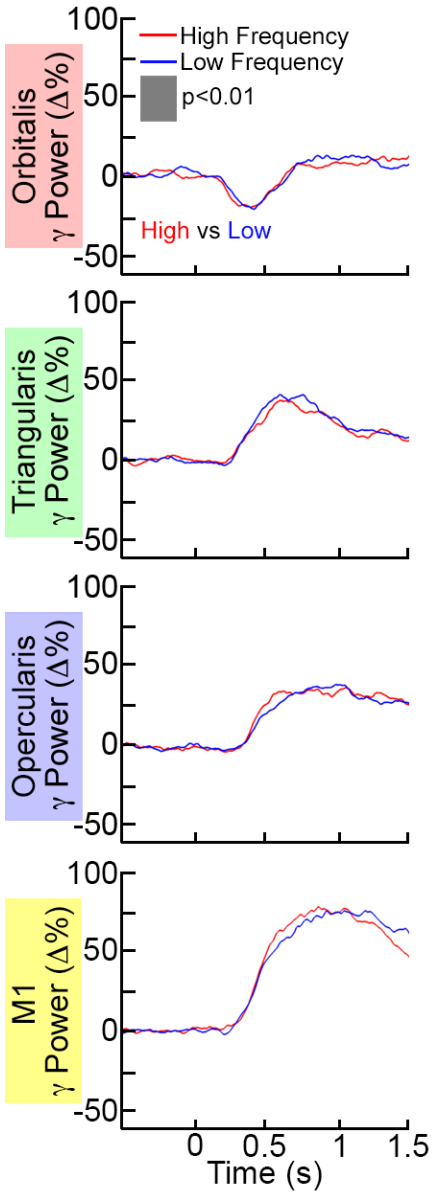

Figure 3.5 Gamma power changes of nouns based on word frequency
Stimuli were ranked by lexical frequency (102) and gamma power changes were computed for each sub-region. No significant differences between the two conditions were noted in any region ($p<0.01$, two-sided, paired t-test, FDR corrected) (from Conner et al 2013 *in review*).

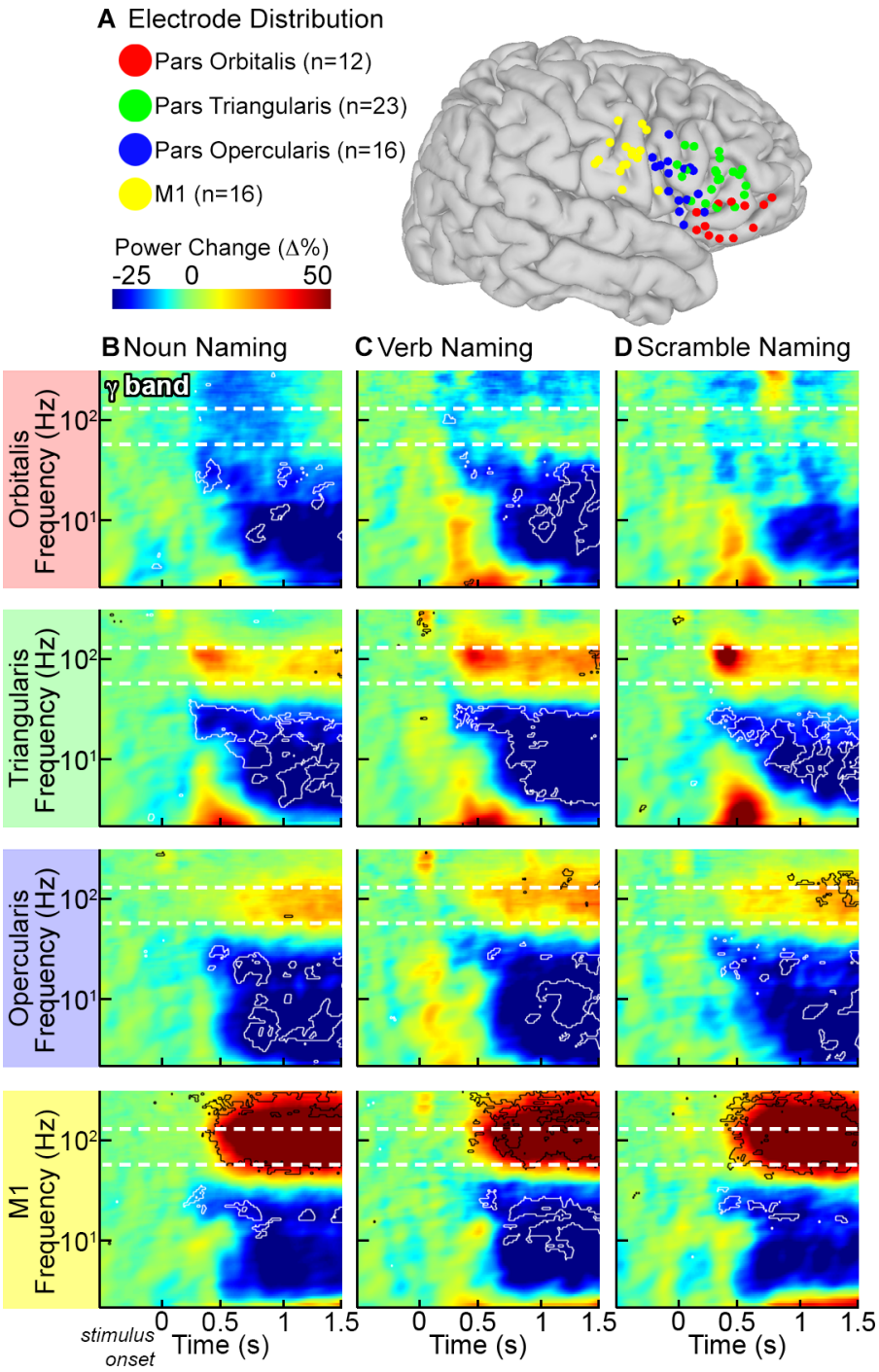

Figure 3.6 Time-frequency analysis of right hemisphere SDEs
(**A**) SDEs from the 10 subjects with right hemisphere data were co-localized on a common brain surface as in Figure 3.3. Grouped time frequency reponses were computed for (**B**) noun, (**C**) verb, and (**D**) scramble naming ($p<0.01$ FDR corrected, two-sided sign test) (from Conner et al 2013 *in review*).

Functional connectivity between all sub-regions was computed using AEC between active SDE pairs for each individual (Figure 3.7) (significance computed using bootstrapping: trial re-shuffling, 1000 iterations) and also across the group (Fisher's z-transform of individual Pearson's r values). Strong pre-stimulus connectivity between POr and PT, and between PT and POp persisted till 300ms after stimulus presentation. Between 300-600ms, a marked negative correlation from POr to PT and from POr to POp was noted ($p<0.01$, two-sided sign-test, FDR corrected) during both noun (Figure 3.8) and verb naming (Figure 3.9), but not scrambled images (Figure 3.10). This corresponded temporally to the decrease in overall gamma power at POr. Baseline bi-directional connectivity between PT and POp was reduced during the same interval and thereafter was principally unidirectional, from PT to POp.

The connectivity of M1 with other LIFG sub-regions was negligible at baseline. Around 400ms, connectivity increased bi-directionally between POp and M1, and lasted till just prior to the onset of articulation of nouns, verbs and scrambled images. PT became strongly, but transiently connected with M1, sending it information between 400-600ms. Just prior to the onset of articulation, M1 became negatively correlated with PT, an interaction suggestive of a stop signal. This pattern of activity was not significant for scrambled images.

POr and POp interactions were weak at baseline, but bidirectional interactions between them started at >750ms and persisted through articulation. Importantly, positive correlation between POr and M1 was significant solely during verb naming (Figure 3.9), suggesting its involvement in processes other than phonologic code retrieval or articulation.

From Conner et al 2013 *in review*

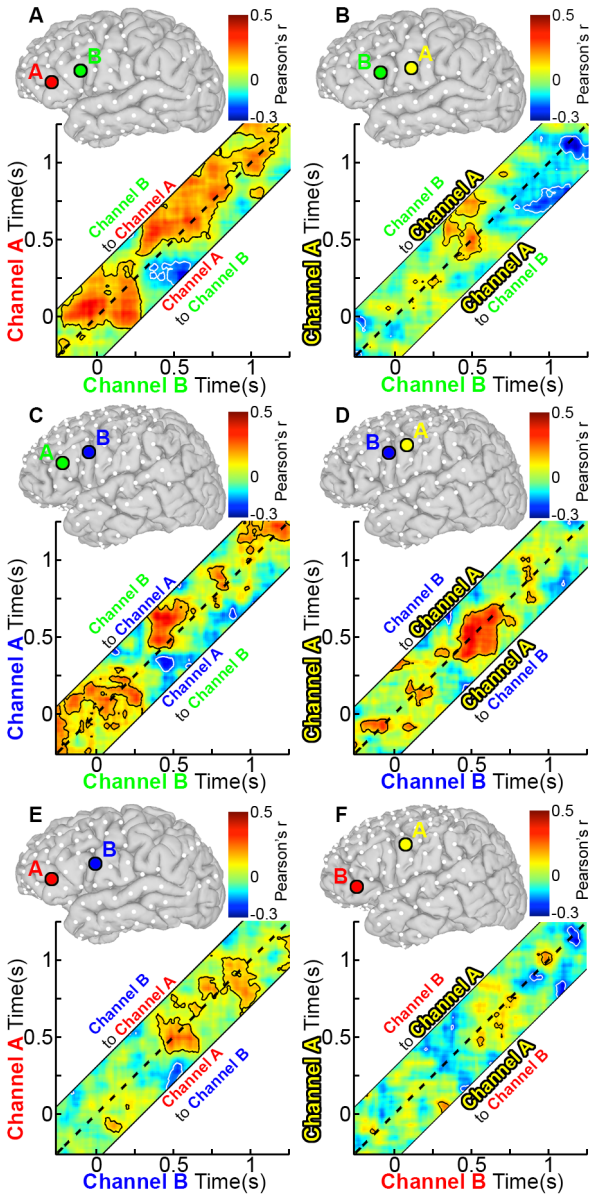

Figure 3.7 Single subject AEC results during noun naming

(**A**) AEC was computed for two SDEs from a single subject over POr (Channel A) and PT (Channel B). The dashed line represents a lag of 0ms, areas above the dashed line represent activity on Channel B correlating with later activity on Channel A, and regions below it lag Channel A before Channel B. Confidence intervals were computed using trial reshuffling (contour lines are $p<0.05$ uncorrected, two-sided, 1000 resamples). (**B**) PT and M1, (**C**) PT and POp, (**D**) POp and M1, (**E**) POp and POr, and (**F**) POr and M1 (from Conner et al 2013 *in review*).

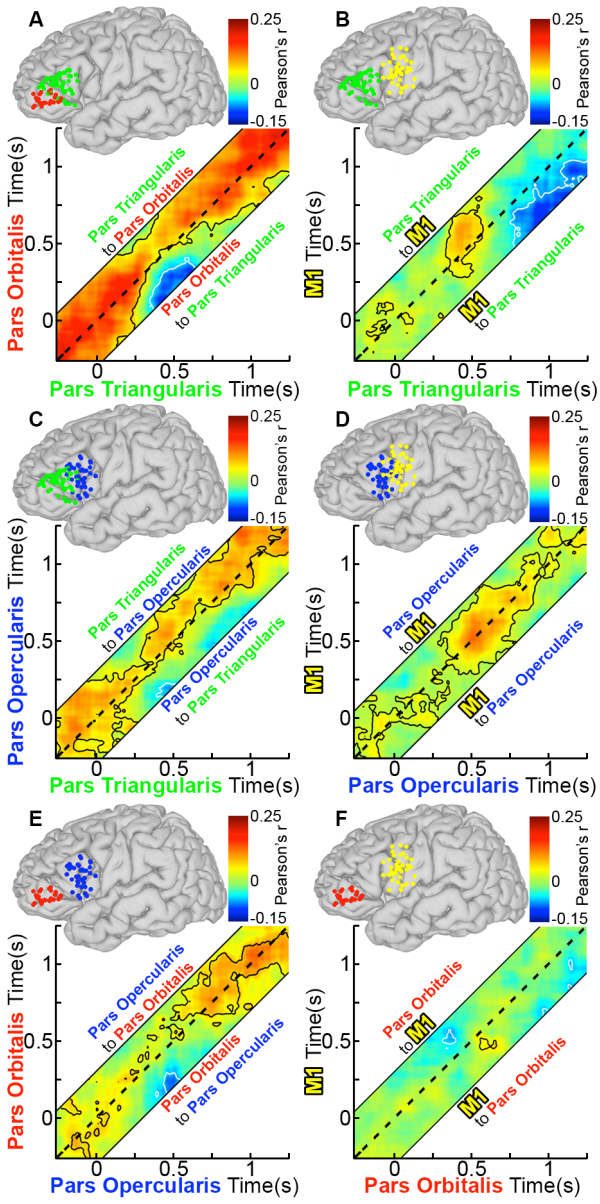

Figure 3.8 Functional connectivity of left IFG during noun naming
(**A**) Grouped PT and POr connectivity was estimated by averaging AEC calculated for each individual (n=28 total pairs of SDEs, contour lines are $p<0.05$, two-sided t-test, FDR corrected). (**B**) PT and M1 (n=39 pairs), (**C**) PT and POp (n=29), (**D**) POp and M1 (n=41), (**E**) POp and POr (n=23), and (**F**) POr and M1 (n=31) (from Conner et al 2013 *in review*).

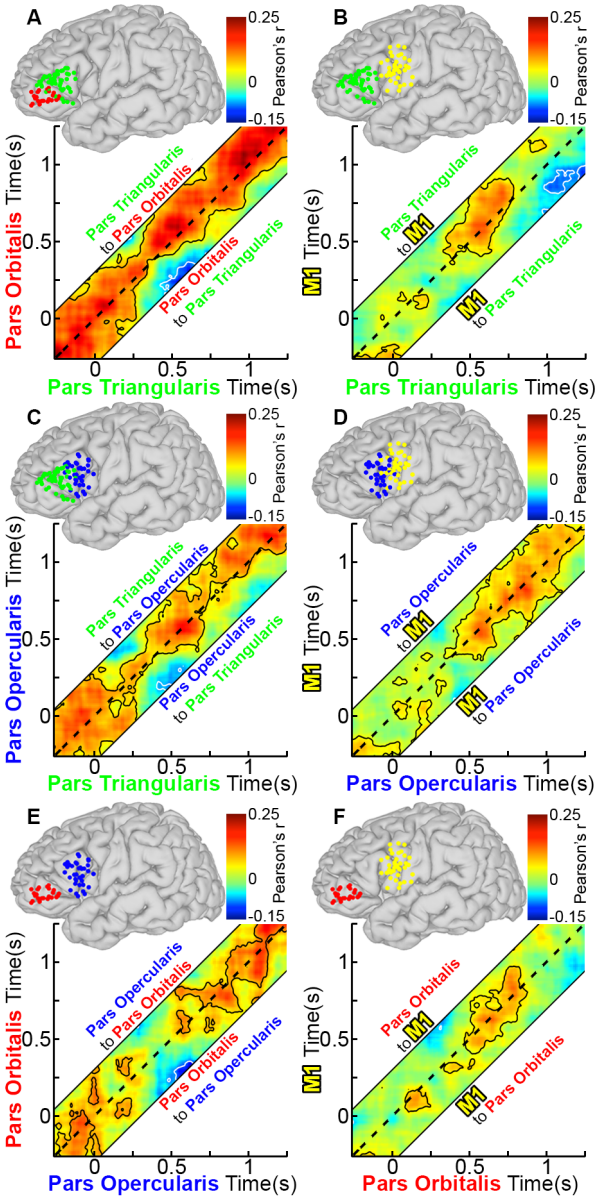

Figure 3.9 Functional connectivity of left IFG during verb naming
(**A**) PT and POr (n=28 total pairs of SDEs, p<0.05, two-sided t-test, FDR corrected), (**B**) PT and M1 (n=39 pairs), (**C**) PT and POp (n=29), (**D**) POp and M1 (n=41), (**E**) POp and POr (n=23), and (**F**) POr and M1 (n=31) (from Conner et al 2013 *in review*).

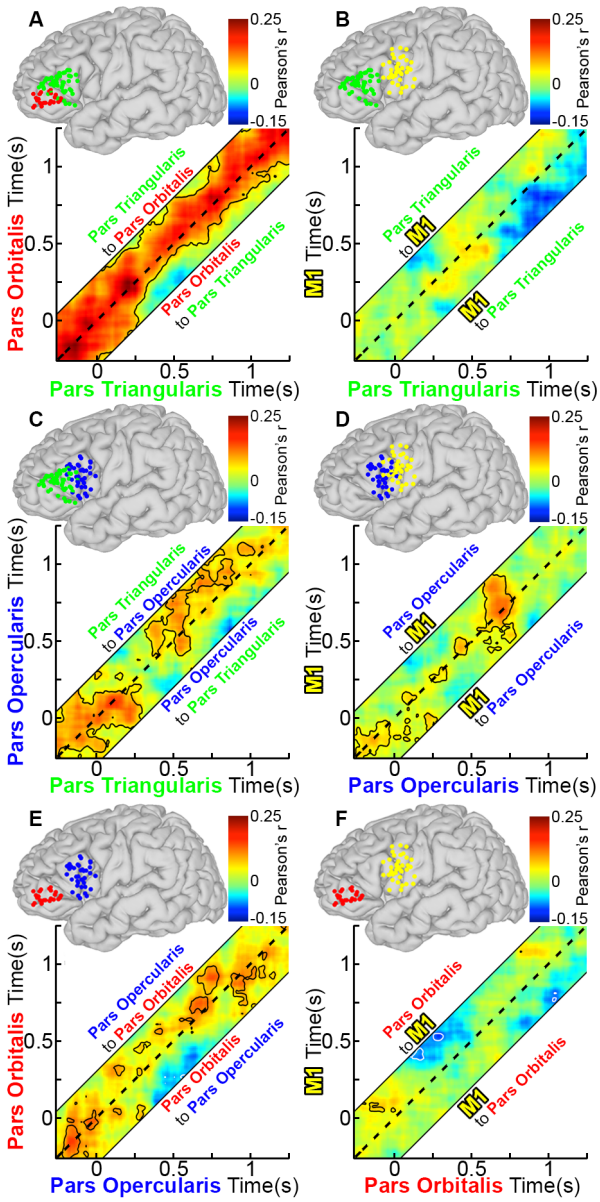

Figure 3.10 Functional connectivity of left IFG during scramble naming
(**A**) PT and POr (n=28 total pairs of SDEs, p<0.05, two-sided t-test, FDR corrected), (**B**) PT and M1 (n=39 pairs), (**C**) PT and POp (n=29), (**D**) POp and M1 (n=41), (**E**) POp and POr (n=23), and (**F**) POr and M1 (n=31) (from Conner et al 2013 *in review*).

Attractor state dynamics were modeled using k-means clustering of the information flow between all regions across the entire time series (125). Similar connectivity patterns were clustered in time and visualized in phase space using principal components (Figure 3.11). During noun naming, five clusters were isolated: baseline and initial processing (pre-stimulus to 300ms post-stimulus), early processing (300-650ms), late processing (650-900ms) and articulation (900-1250ms). Based on the profile of these clusters, a spatio-temporal schematic for these states was constructed, with edges representing inter-nodal connectivity and size representing activation. Analysis of scrambled naming demonstrated a return to rest at 1.25s due to shorter latency of articulation (Figure 3.12). Verbs had a vastly similar state pattern to nouns, but included an additional metastable state near the end of early processing (400-650ms). This additional attractor likely represents interactions of M1 with POr and PT.

The connectivity of IFG sub-regions was also evaluated as a function of noun frequency and selectivity. The negative correlation from M1 to PT was greater for high vs. low frequency and for low vs. high selectivity, reaching maximum significance around 790ms after stimulus offset ($p<0.01$, paired t-test) (Figure 3.11). This negative feedback coincides temporally with the maximal difference in activation between high and low selectivity nouns in PT and POr.

From Conner et al 2013 *in review*

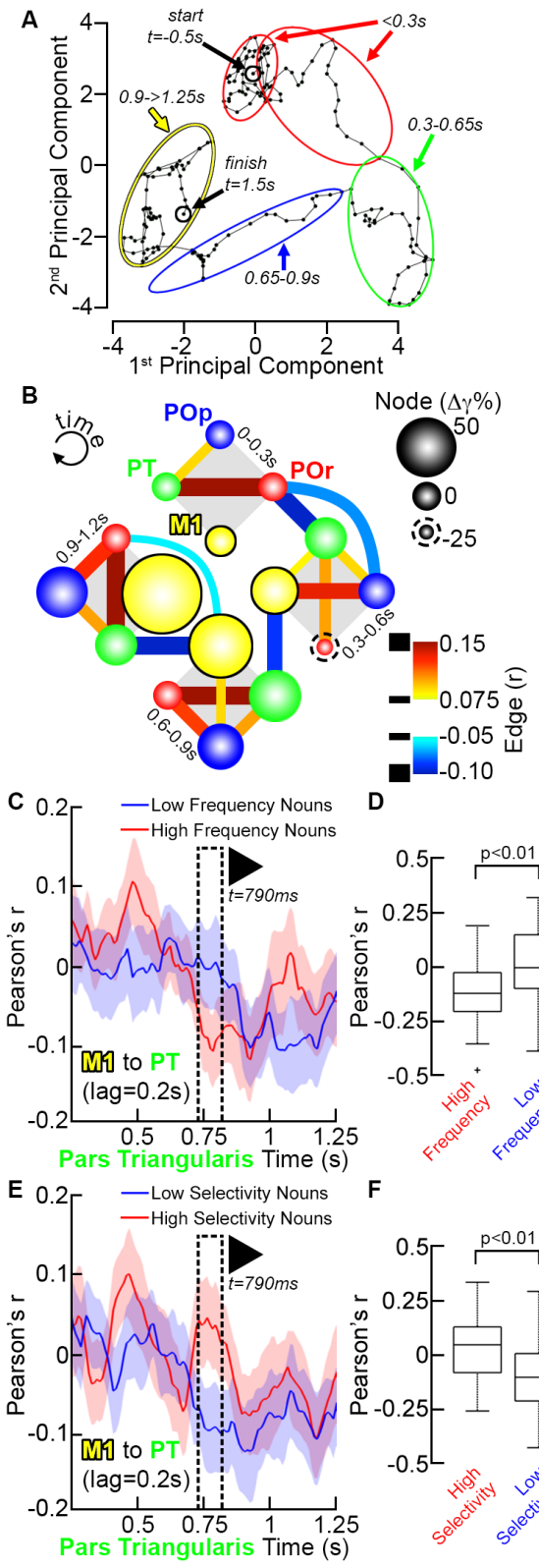

Figure 3.11 LIFG dynamics of functional connectivity during noun naming
(**A**) K-means clustering of AEC results into groups of time points. Five clusters were identified by the analysis and projected along the first two principal components (accounting for 50% of total variance). (**B**) Schematic of network dynamics, edges represent inter-nodal connectivity and size represents activation (gamma power) of each sub-region. (**C**) Functional connectivity of high and low lexical frequency (102) nouns between PT and M1 were computed (M1 to PT, lag=0.2s, mean +/- 2 sd, n=39 SDE pairs). (**D**) AEC of high frequency at 790ms was significantly less than low frequency ($p<0.001$, two-sided, paired t-test). (**E**) and (**F**) High and low selectivity compared using the same analysis (from Conner et al 2013 *in review*).

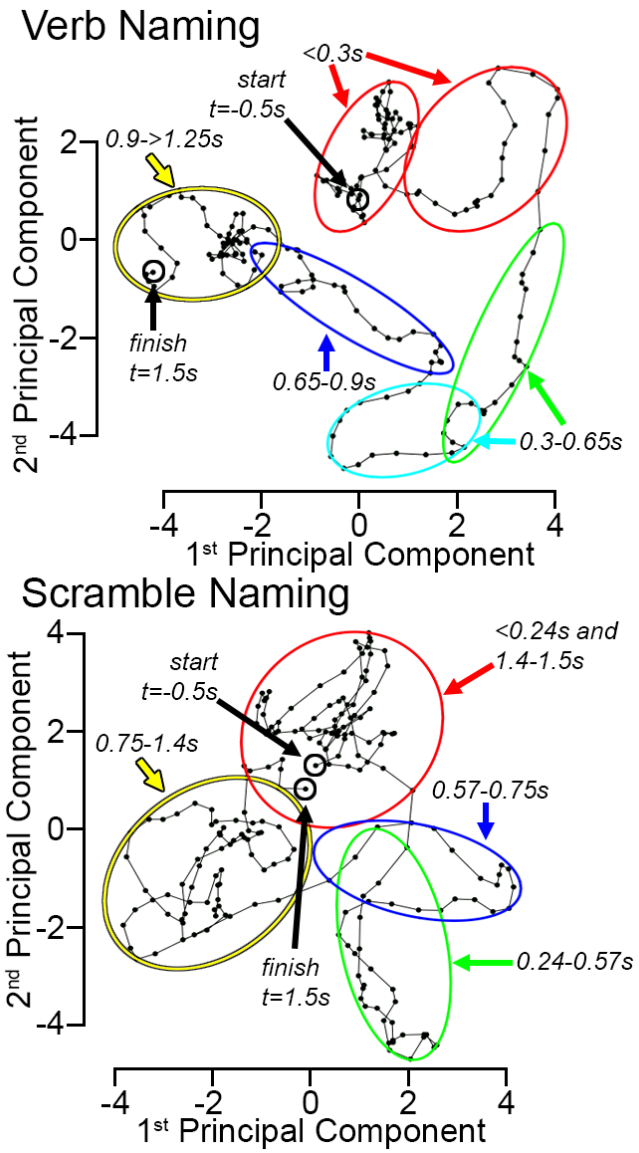

Figure 3.12 LIFG temporal dynamics during verb and scramble naming
K-means clustering of AEC results into groups of time points. Five clusters were identified by the analysis and projected along the first two principal components (accounting for 50% of total variance) (from Conner et al 2013 *in review*).

Conclusions

We found that 300ms after stimulus onset, POr gamma activity decreases while a strong, negative correlation from POr to PT is present. One interpretation is that the normal excitation-inhibition balance between these areas favors positive correlation at rest, and that during initial language processing this balance is adjusted towards greater inhibition. This could be caused by decreased activity in POr neurons responsible for exciting PT, and would account and both the gamma decrease and negative correlation. Previous work using pharmacological manipulation found that changes in the excitation-inhibition balance had significant effects on reaction time in language generation tasks (128), suggesting that such inhibition plays an important role in processing.

System state analysis showed that the first attractor that the network enters into is defined by the inhibitory POr shift (Figure 3.11), implying that this phenomenon may act to initiate language processing by forcing this dynamic system out of rest and into the first processing state (125, 129). Prior fMRI and lesion work have implicated POr and PT in the processes of controlled retrieval and response selection, respectively (54-56). Under this model, POr is thought to assist semantic processing through top-down activation of association cortex, while response selection uses competitive dynamics and lateral inhibition to isolate the most active possible response (57). Given that response selection necessarily acts upon the results of controlled retrieval, one possible explanation for the mechanism of controlled retrieval is inhibition of response selection that we observed (58). This

would result in decreased inhibitory drive in PT, and account for the observed functional connectivity between POr and association cortex during naming.

Two other models of PT functionality, the domain specific (59, 60) and domain general models (61, 62), hold divergent views regarding whether phonology and semantic processes occur in distinct modules in POp and PT or whether these operations overlap in PT. In the scrambled naming tasks, subjects accomplished several sub-goals, including visual processing, rule monitoring, and phonology; however, semantic processing was not required. Any region engaged in phonology should be significantly active during scrambled naming, however, PT was not (Figure 3.4). This is in contract to POp, which was active during all three tasks, and was not modulated by the degree of selectivity of the response. These finding imply that POp is involved in intrinsically different processes than PT and directly supports the domain specific model of the LIFG. Importantly, given the early activation of POp, it is clear that phonological access occurs in parallel to the processes of controlled semantic retrieval and response selection. Such a finding may explain why no significant difference in activation was found between high and low frequency nouns despite the presence a word frequency effect (15). Although, this could also be explained attributed to different processing times in regions that were no recorded from, most notably the anterior insula (130). If the phonological forms of the responses are activated early and in parallel, then activation patterns may not be significantly different.

Activation of M1 was also investigated to test the motor theory of language, a framework postulates that M1 is crucially involved in semantic processing of action

associated words (e.g. verbs) (31). When examining M1 interactions with LIFG, we found significant M1 functional connectivity to POr only during verb naming (Figure 3.9). Given that POr is thought to mediate semantic processing (54), information flow between these regions possibly reflects additional processing not required for noun or scramble naming and is manifest in the metastable attractor state seen only in verb naming (Figure 3.12). It is unlikely to represent increased phonological demands due to its absence from both noun and scrambled naming. Given that visual demands and response profiles were similar across conditions, it possible that this additional state reflects increased semantic processing or syntax. Although it is not possible to prove this assertion with this dataset given the low syntactic contrast between these conditions.

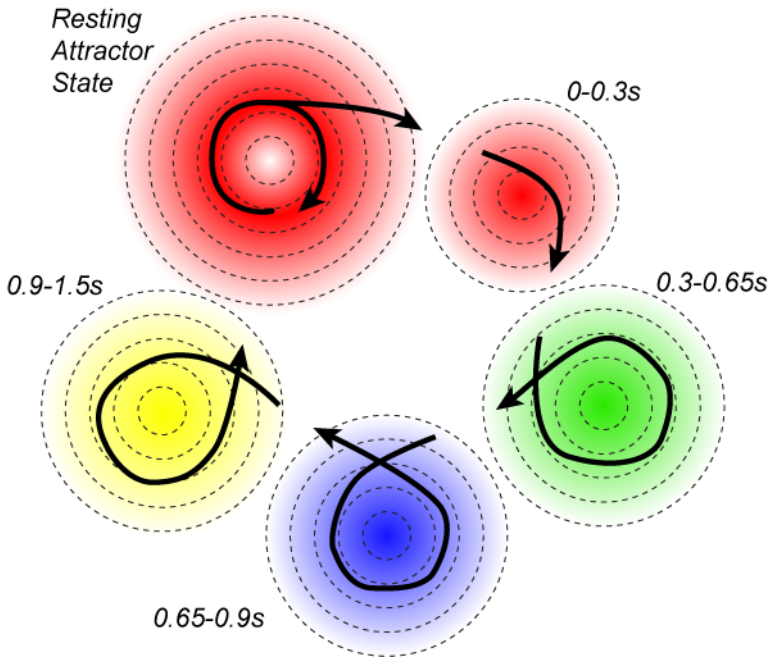

Figure 3.13 Attractor state model for noun naming
Five states were identified. The first, a periodic attractor state, is indicative of the system at rest. At stimulus onset, the system is moved out of this state and proceeds across four point attractor states before returning to rest. Color and time epochs are derived from Figure 3.11.

The interactions between these regions rapidly change in time, magnitude, direction, and valence. These results show that the system cannot be described as strongly hierarchial because it does not display strictly serial activation profiles, rigid feedforward-only interactions, or rostral-caudal dominance relationship, all of which are characteristics of hierarchical processing (63, 66, 131, 132). In particular, our work revealed an ascending control signal from POr to PT signaling the start of lexical processing, and a descending one from M1 to PT that terminates it (64). The onset (but not magnitude) of the M1 to PT interaction was significantly earlier for high frequency and low selectivity words, implicating it in this role (133). As POr appears to control the start of lexical processing, the positive correlation between POr and POp that occurs when PT is engaged in response selection may serve as the final arbiter of system readiness that initiates articulation. These results shed some light on the functionality of LIFG, may be used in future models of this regions role in language generation.

Limitations and Alternative Explanations

This study focused on the gamma (70-110Hz) frequency range for both activation and information flow analyses. The neural generator of the gamma signal is an area of intense physiological research. And while understanding it is important in spatio-temporal descriptions of activation, it is paramount in network analysis because the interpretation relies on the relationship of two populations with one another. The AEC method employed here assumes that gamma power coupling is a reliable indicator of information flow, however, this may not necessary be the case (134-136). Gamma oscillations themselves are thought to arise from peri-synaptic potentials (137). Regions coupling as a large-scale neuronal ensemble should have some correlated firing patterns over time due to communication between them (138). This correlation is thought to result from information flow between the two regions; increased action potentials from one region impinging on another increasing activity there. As increases in gamma activity may or may not reflect increased processing, the presence of envelope correlations may not reflect information flow.

The gamma frequency range was chosen due to rapid signal attenuation (<6mm) caused by high SDE impedance and low signal amplitude (2-5microVolts for the 70-110Hz band). As an added control, we used noise correlation as our measure of functional connectivity. The small fluctuations used to calculate AEC presumably have even greater fall off and would therefore be even less susceptible to common sources as drivers of the observed correlations (139). Importantly, the presence of both negative and unidirectional correlations in the results argues

against the influence of common cortical sources. Such asymmetries suggest that common cortical sources are not an issue with these data or this analysis. However, these assertions may not hold for lower frequencies because signal power is much higher and has greater spatial distribution. Given the importance in lower frequencies in establishing long-range communication (135, 136), it stands to reason that these frequency bands would be of interest in future analysis. One possible solution would be to use signal orthogonalization to ameliorate contamination from a single, common source, although this greatly underestimates overall connectivity (Hipp 2012, J.F. Hipp personal communication October 2012). Furthermore, in many cases only a single contact was present in the regions of interest, necessitating a common average reference, but excluding coherence and Granger causality as measures of functional connectivity.

As in all information flow analyses, it is necessary to acknowledge that the connectivity noted in these results could possibly be the result of a third, un-recorded neural substrate. Interactions between regions could be the result of a common input to them, or information flow from one region to another could traverse through an intermediate structure that was not sampled. None of the patients that were included in this study had electrophysiologic recordings from sub-cortical structures, most notably the basal ganglia. The function of these structures in language processing and their effect upon cortical activations and inter-areal dynamics is poorly understood at this time (140, 141). One specific alternative to our interpretation of the negative correlations could involve both the globus pallidus and the dorsal striatum as a mechanism of inhibition (Figure 3.14). The current de-

exciation model that argues for feedforward inhibition could also be explained by a loop involving increased inhibition within the basal ganglia (reminiscent of the indirect pathway of movement). Dissociating between these possible explanations may be difficult, although neuroimaging (fMRI and MEG) could offer a solution. Alternatively, the use of pharmacology to selectively modulate different systems during ECoG recordings could also be used; this assumes that the neurotransmitters used by the cortico-cortial and coritco-subcortical-cortical paths may be different. If the patients are asked to perform the same tasks just prior to surgery (when anesthetics are administered), the augmentation of different neurotransmitter activity is possible. Furthermore, to investigate the involvement of sub-cortical areas, future work should involve analysis of different frequency bands as they may facilitate interactions between the cortex and these areas (142).

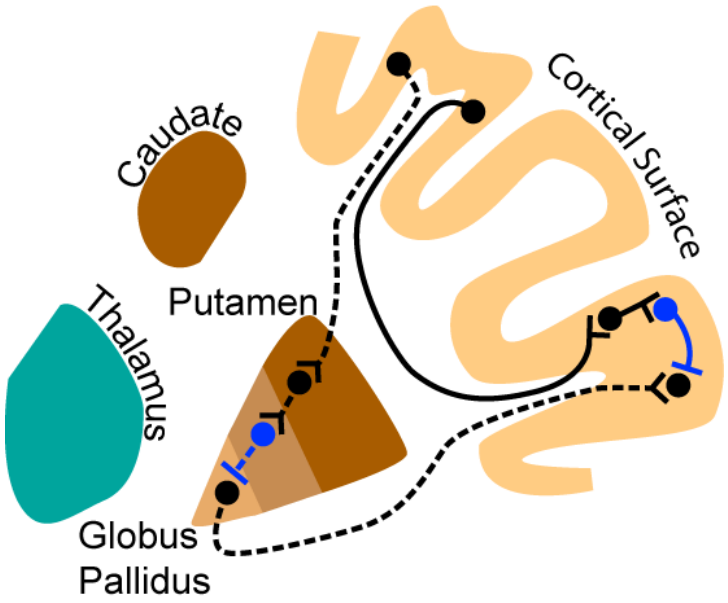

Figure 3.14 Two possible explanation of observed negative correlations
Negative correlations between regions (such as POr and PT/POp, or M1 and PT) could be mediated by several possible mechanisms. Feedforward inhibition (solid line circuit) could use excitation of local interneurons in the target region to directly modulate firing. A possible sub-cortical alternative (dotted lines) could be inhibition of excitatory drive of the target area via interactions between the globus pallidus and the putamen and/or the caudate.

Positive correlations observed between these regions were found to occur over a wide range of latencies, both in the tens and hundreds of milliseconds. In many cases, these positive correlations were bi-directional. Our interpretation of these results was that these areas were directly coupled with one another, regardless of lag. One underlying assumption was that these regions are located closely enough together that they there is no intervening region between them through which they communicate. A second assumption was the common input to these areas was not the main reason for observing these correlations. It is certainly possible that ascending input of earlier processing (in temporo-occipital cortex) may be the real explanation for this functional connectivity. However, if this were the case, we would have expected to see earlier increases in bi-directional connectivity (reflecting the arrival of common input to these areas near the same time) and no unidirectional connectivity. In reality, we found neither of these to be true – the onset of connectivity was heterogenous and there were multiple instances of unidirectional connectivity (including negative correlations). While the overall activity of PT, POp, and M1 did increase at roughly the same time (reminiscent of common input), the interactions between were idiosyncratic. The remaining possibility is that the ascending input may have different influences on each region that are not strictly positive. With the current work, this final alternative cannot be completely rejected.

Examining these alternative interpretations could progress through several different avenues. The current work is limited by the exclusion of distant cortical structures and a lack of sampling of sub-cortical regions. The first step in future

work is to examine how temporo-occipital areas feed information into prefrontal cortex. These regions provide the input into the system, and could certainly drive the positive correlations that were observed through common input to several areas. It would be interesting to seem how POr and PT, in particular, interact with these areas given their presumed roles in controlled retrieval and response selection. If some prefrontal structures are found to functionally couple with temporal and occipital regions while others do not (or if the pattern of there connectivity is not homogenous), this would support the claims that these regions are carrying out different functions and that the influence of common input on intra-Broca's area connectivity is less significant than presumed. Given that PT, POp and M1 share a similar timing of activation while POr is quite different, we would expect at least some variation in network dynamics.

Inclusion of event-related fMRI in the study of regions that are rarely sampled with invasive human electrophysiology could also investigate the roles of these neural substrates in the observed network interactions. fMRI has the advantage of greater coverage at the cost of temporal resolution. Using a technique such as dynamic causal modeling, it is possible to directly compare models using a Bayesian framework (143-145). The argument that other regions might be involved (including sub-cortical or insular areas) would be compared with the current explanation – that these areas communicate directly. One important caveat is that many of the observed changes in inter-areal connectivity occur at a time resolution below that of fMRI (changes may last <300ms compared to a resolution >2x that). This may limit the power of fMRI to replicated the observed functional connectivity

and fail to delineate between the models described above. Another possibility is the use of MEG for the same analysis. This would circumvent both the spatial and temporal issues of ECoG and fMRI, respectively. However, despite the potential to resolve many different sources simultaneously, there are considerable issues with common source contamination. This necessitates the use of orthogonalization or source separation calculations, both of which cause substantial underestimation of functional connectivity (123).

Ultimately, none of the aforementioned techniques can solve these issues alone. An addition issue to the tradeoffs between coverage, temporal resolution, and source separation is the continued lack of understanding of how different frequency bands contribute to inter-areal communication (135, 141). One of the strongest alternatives to the current interpretation is the involvement of sub-cortical structures, yet there is little understanding for how these regions are involved in language (142). Saliently, we have an imperfect knowledge regarding the frequencies used to facilitate interactions between sub-cortical and cortical structures. The difficult, but necessary solution, involves combing results from data of several different types (i.e. ECoG, stereo EEG, MEG, fMRI) and computation modeling to resolve the new questions raised by this work.

CHAPTER 4: CONCLUSION

In our study of language, we collected ECoG data from a large cohort of subjects during three visual naming tasks. Our goal was to investigate the dynamics of neural activation during these tasks to determine the structure and order of processing. To accomplish this task, new methods of group analysis were developed and used with robust measures of functional connectivity. This work primarily addressed three questions regarding differences between verbs and nouns in the mental lexicon, the functions of the LIFG, and the serial or parallel nature of language processing.

The first question that we addressed dealt with the organization of nouns and verbs within the mental lexicon. Our hypothesis was that there are differences between nouns and verbs that exist along the ventral and dorsal streams, respectively (the dual stream hypothesis). Group analysis of these results revealed clear dissociations, especially in parietal cortex, which was much more active for verbs. Sub-temporal cortex was significantly active for both tasks, although to a greater extent for nouns. This distinction was greatest for the PHG, which was only significantly active during noun naming. These results confirmed the original hypotheses, and were in support of the spreading activation model and the motor theory of language.

Subsequently, we examined the roles of Broca's area and LIFG in language processing, and the extent to which this area is recruited for both language tasks. Our results were largely in agreement with the two-process theory, and revealed that PT was the only sub-region whose activity was modulated by response selection. We also found that POr deactivated near stimulus onset, while exerting

significant control over both PT and POp. These findings suggest that this POr may halt response selection to allow for semantic processing, and may be the mechanism for controlled retrieval. However, the descending interactions of POr with posterior LIFG were mirrored by the ascending feedback control from M1 to PT near the onset of articulation. This demonstrated that the hierarchy of LIFG was not strictly rostro-caudal, and involved posterior regions sending feedback forward to more anterior ones.

Our final goal was to characterize the topology of processing to delineate between the parallel distributed processing model, or the serial heiarchy of language production. We found that initial processing in visual and sub-temporal regions began at roughly the same time point (around 100ms after stimulus onset), whereas prefrontal cortex was not active until much later (400ms). However, within these two time windows, the constituent regions appeared to operate in parallel. ITG, PHG, fusiform and lateral occipital cortex had a similar onset of activation, regardless of stimulus type. In LIFG, initial deactivation of POr was followed by concurrent activation of the remaining sub-regions (PT, POp, M1). These findings suggest that there may be a two-tiered hierarchy of activity: first, visual and semantic processing occur in parallel, and second, the functions of LIFG are carried out concurrently prior to articulation. Future work will need to utilize the network analysis used in the second goal to incorporate the interactions of temporo-occipital cortex with the LIFG. Until there is a more complete description of how these regions connect to POr and PT during speech production, it is not possible to completely confirm or reject this hypothesis.

Significance

The novelty of this work lies in both the type and volume of the data that was collected for language studies, the techniques that were applied, and the implications of results that were produced. Typically, ECoG studies of language consist of a handful of patients (<10) and may or may not incorporate functional neuroimaging. By utilizing a large cohort of individuals in whom we collected both of these datasets, we were able to leverage the power of fMRI (near-complete sampling of the cortex) and ECoG (high temporal resolution and high signal-to-noise ratio) in a single group of subjects. We used this to make comparisons between these modalities, compare statistical power for grouped analysis, cross validate our results, and relate our work to the neuroimaging literature (1, 68). However, this would not have been possible without first developing a novel method for population level analysis of ECoG datasets. Before this was completed, such methods were under-developed and lacked statistical rigor. The mixed-effects multilevel analysis used here will be used in several future projects and is also available to other groups.

In the first experiment, we demonstrated that nouns and verbs somewhat differ in the areas of cortex that are involved in their processing. While this result has been predicted by several lesion and neuroimaging studies (38, 48, 74, 146), this has remained an unresolved question in the literature (67, 75, 76, 78). Our results provide additional support for dual stream hypothesis. Perhaps more importantly, the finding that activation is neither completely parallel nor rigidly serial has important implications for the continued development of models of language

production. The fact that processing appeared to progress in two stages that were internally parallel disagrees with many of the contemporary frameworks (13, 15, 19, 39, 147). Substantial re-structuring of these models will need to occur if they are to account for the findings of this work.

Our subsequent network analysis of Broca's area dynamics was used to examine several different theories. These included the two-process theory (54), domain general/specific processing in PT (61), and the motor theory of language (31). The description of the functional specialization of the sub-regions of LIFG and the inter-areal interactions was a significant advance over the current research. We were able to validate and refine the two-process theory because of the high-temporal resolution of the data and the use of a powerful analytic tool (AEC). We also found that both the domain specific and motor theories were consistent with our data. Both have remained controversial due to conflicting reports, the resolution of these debates will effect future studies of action perception, the organization of the mental lexicon, and phonological encoding. Validating these theories has been difficult using fMRI and its limited ability to resolve network interactions at small time intervals. Finally, the novel application of attractor state dynamics to argue against a rostro-caudal hierarchy of prefrontal cortex has far reaching implications for many fields, notably executive control (131, 132).

Future Directions

While this work does shed some new light on language processing, significant work remains. The use of visual stimuli allowed for consistent timing of activation in all subjects. However, it meant that studying other input modalities,

most importantly auditory language stimuli, was not considered here. This limited the possible questions regarding the mental lexicon that might have been addressed. Future work should employ the methods used here to analyze auditory naming tasks, data that has already been collected in conjunction with this work. Such research would be able to answer questions about the possible overlap between modalities, and may even be able to answer the dual coding hypothesis (103, 148-150). This question deals with the overlap between semantics used to process different input modalities. It specifically delineates between models that have a common mental lexicon for two different sensory processing streams (auditory and visual), and those that do not. The use of group activation and network flow analysis would be able to determine if such areas of convergence exist, or if language processing for different input streams remain separate.

The network interactions observed involved both positive and negative correlations. Given the importance of the excitatory-inhibitory balance on naming (in particular to the response selection component), it would be useful to examine how these interactions change under the administration of pharmacological agents (128, 151). The use of GABA-agonists has been shown to aid in response selection, presumably via increased lateral inhibition. However, their effect on the functional connectivity between POr and PT, POr and POp, and M1 and PT would help to clarify whether the negative correlations are the byproduct of feedforward inhibition or de-excitation. While pharmacological manipulation may not be feasible extra-operatively, all subjects undergoing invasive electrophysiology must have an operation to remove the implanted electrodes. At the time of this operation, the

patient is given benzodiazepines in preparation for surgery. It may be possible to record ECoG data both extra-operatively and intra-operatively in a select group of patients and to analyze how these drugs affect functional connectivity within the LIFG.

Direct electrical stimulation offers another possible route to investigate the function and interactions of these regions. Such stimulation is routinely performed on these patients as a means to map out eloquent cortices before surgical resection (96, 152). Using limited stimulation applied to these sub-regions, the disruption or augmentation of function in a time-locked and double blind fashion is possible (153). This is in contrast to trans-cranial direct current stimulation or trans-cranial magnetic stimulation that have poor spatial targeting and often induce painful muscle contractions that preclude a blinded experimental setup. A preliminary study might include stimulation of POr to monitor for the effects on response selection (through the interaction with PT) and error rates.

Summary

The production of speech in response to a visual stimulus requires the integration of perceptual, semantic, and phonological processes (86). Rather than dissociate between semantic syntactic and phonologic processes using subtractive paradigms, we sought to evaluate the interplay between these processes during fluent naming. Our results reflect a new model of visual naming starting with initial visual and semantic processing in ventral temporo-occipital cortex that begins ~100ms after stimulus onset (1). Shortly thereafter, POr de-activates, presumably due signaling from ventral temporo-occipital, and inhibits PT and POp via de-

excitation. This process stalls response selection and phonology until ventral temporo-occipital processing has sufficiently progressed, and may be crucial to controlled retrieval. The middle processing state starts at 400ms, when LIFG activity constitutively increases. PT uni-directionally drives M1 and POp, while bi-directional interaction between these M1/POp increases for all tasks in order to complete phonologic retrieval. Around 600ms, LIFG enters the late processing state as inhibitory drive from POr decreases and it functionally couples with POp, and additionally to M1 during verb naming. At the same time, response selection demands are greatest, and POp/PT are strongly functionally coupled. These findings suggest the involvement of POr in arbitrating readiness of articulation. Finally, M1 terminates lexical processing in PT and the system returns to rest. In this model, POr is central to the timing of retrieval and state transitions, PT is essential to resolving semantic ambiguity (57), and POp/M1 address the demands of phonology and articulation.

We have found that while there appears to be two stages of processing that occur in sequence, the sub-processing within them occurs in parallel. Initially, sensory and semantic functions activate near the same time point, although there are differences in how words of different grammatical classes are processed. After this initial processing, LIFG carries out the functions of response selection (PT) and controlled retrieval (a result of POr and PT interactions), phonology (POp is largely responsible) and articulation. Using these new techniques and exciting data, it may be possible to build a more complete model of language perception and production,

and eventually construct brain computer interfaces for individuals that have lost this essential function.

APPENDIX: Amplitude Envelope Correlations

We chose amplitude envelope correlations as our measure of functional connectivity for several reasons. Unlike other methods such as coherence or Granger causality, AEC works regardless of signal stationarity or heteroskedasticity (120, 122, 123, 154). Compared with Granger causality, it is substantially less sensitive to noise from a common source (AC line artifact) and any filtering done as a result its presence, and can be applied when different referencing schemes (including a common average reference). This technique can also report coupling at arbitrary time lag and can depict the changes in magnitude, direction and valence with high time resolution and without dependence on windowed analysis. These advantages come at the cost of specifying a number of parameters before analysis, namely the frequency bands of interest and any smoothing that will be applied to the signal envelope. However, with ECoG data, the frequency band of interest for language processing can be defined as the middle gamma band (70-110 Hz) with some degree of confidence (68, 155-160).

Equations

A noise correlation between pairs of channels was computed with the Pearson's correlation at each time point across trials. With ECoG data, the signal (x) is first fast Fourier transformed (FFT) into the frequency domain

$$X = FFT(x) \tag{1}$$

Filtering and the Hilbert transform are performed in the frequency domain using a single transfer function *H(s)*

$$X_f = X * H(s) \quad (2)$$

Applying a reverse Fourier transform results in the analytic signal ($x_f(t)$) for that frequency band

$$x_f(t) = iFFT(X_f) \quad (3)$$

The absolute value of this can be used to compute the instantaneous amplitude envelope ($A_f(t)$) for that frequency band

$$A_f(t) = |x_f(t)| \quad (4)$$

The amplitude envelope is then smoothed by convolving it with a moving average filter (MA(l)) with length l ms (100ms for the 70-110Hz band) (161)

$$A_{signal,f}(t) = A_f(t) \otimes MA(l) \quad (5)$$

For AEC, a noise correlation between channels is used. The first step is to subtract the average of the envelope at each time point, $E(A_f(t))$, from the each individual trial to get the variance, $A_{signal,n,f}(t)$

$$A_{noise,n,f}(t) = A_{signal,n,f}(t) - E[A_f(t)] \quad (6)$$

Then a Pearson's correlation,

$$\rho = \frac{E[(X - \mu_X)(Y - \mu_Y)]}{\sigma_X \sigma_Y} \quad (7)$$

Is used to calculate the correlation between two signals, *A* and *B*, for each time point, *t*, using all *n* trials as the individual observations

$$\rho(t) = \frac{E[(A_f(t) - \mu_A)(B_f(t) - \mu_B)]}{\sigma_A \sigma_B} \quad (8)$$

Significance of this correlation is computed using bootstrap reshuffling of trials to generate additional observations of ρ. The associated p-value is then the proportion of resamples that lie a greater distance from the median.

Given that this calculation is not dependent on the band that is used, it is possible to compute both cross-frequency coupling and phase-amplitude coupling (using the analytic signal to calculate instantaneous phase) (135, 162). If single unit data were recorded, the instantaneous firing rate could also be used as one of the envelopes used in the AEC calculation (163-165). Furthermore, the time point that for each channel does not necessarily have to be same. The correlation between two signals can be computed at any given lag and then assigned a significance level as though they were from the same time point. This allows for a rudimentary estimate of directed information flow.

Simulations

The AEC algorithm was tested using simulated data of three Poisson cells. Two cells fired independently at two different rates (30 and 50Hz) (166, 167). A third cell, firing at 10 or 30Hz, was a common source of input to both cells, such that when it fired at a given time point, each of the other cells was guaranteed to fire. For each simulation, 100 trials were randomly generated each with a length of 1000ms, and the common input was supplied to both cells from 250 to 750ms. Instantaneous firing rate was calculated by convolving each trial with a Gaussian function (sigma = 20ms). AEC was calculated as described above (significance was calculated using 250 resamples).

For the first simulation, common input firing at 30Hz was supplied to both cells with 0ms lag between them. Firing of both cells increased dramatically during the period of common signal input (Figure Appx.1). Before and after this epoch, correlations between the two cells were relatively low. From 300 to 700ms, there

was significant ($p<0.05$), positive correlation at 0ms of lag, validating the methodology and the simulated data.

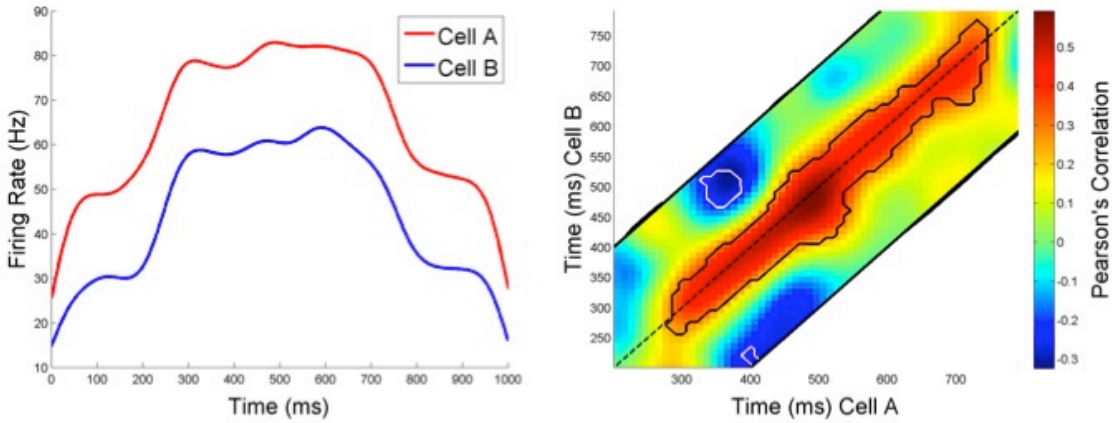

Figure Appx.1 Zero lag connectivity
Two Poisson cells, one with an intrinsic firing rate of 50Hz (Cell A) and another with a firing rate of 30Hz (Cell B), are driven by a common source at 30Hz. Each cell receives the input at the same time point (lag = 0ms) from 250 to 750ms. In the AEC plot, correlations away from the 0ms diagonal (dotted line) represent correlations at high lag. Significant ($p<0.05$) connectivity is outline with black (positive correlation) or white (negative) contours.

This simulation was then re-run but with a lower level of common input (10Hz). Under these conditions, the increase in firing rate for both cells was negligible and there was no significant connectivity between the two cells (Figure Appx.2).

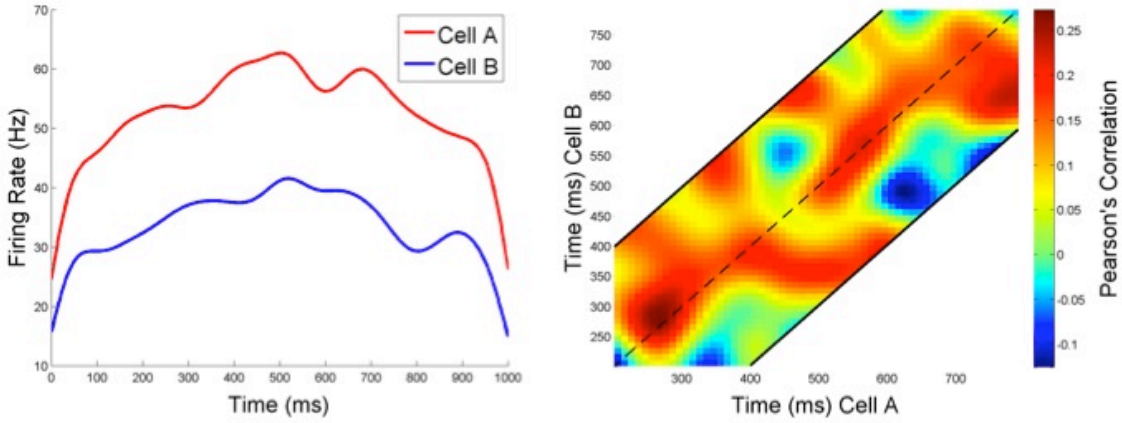

Figure Appx.2 Weak connectivity
If the rate of the common input is lowered to 10Hz, the degree of connectivity drops below the threshold for significance. This shows that only robust connectivity will survive the bootstrap procedure.

Finally, a lagged correlation between the two cells was simulated by delaying the input of the common cell to only one of the cells. The same input signal was applied to both cells for a given trial, but it occurred from 0 to 500ms for cell B, and from 250 to 750ms for cell A. In this way, firing of cell B occured before cell A and causing the direction of information flow to go from cell B to cell A. We found that the 0ms lag correlation was no longer present in this case, despite significant increases in cell firing (Figure Appx.3). A significant, directed information flow from cell B to cell A was seen that started near the beginning of the time epoch and persisted until around 700ms. This connectivity was noted at a lag of 250ms, reflecting the design simulated data and demonstrating how directed information flows can be calculated with AEC.

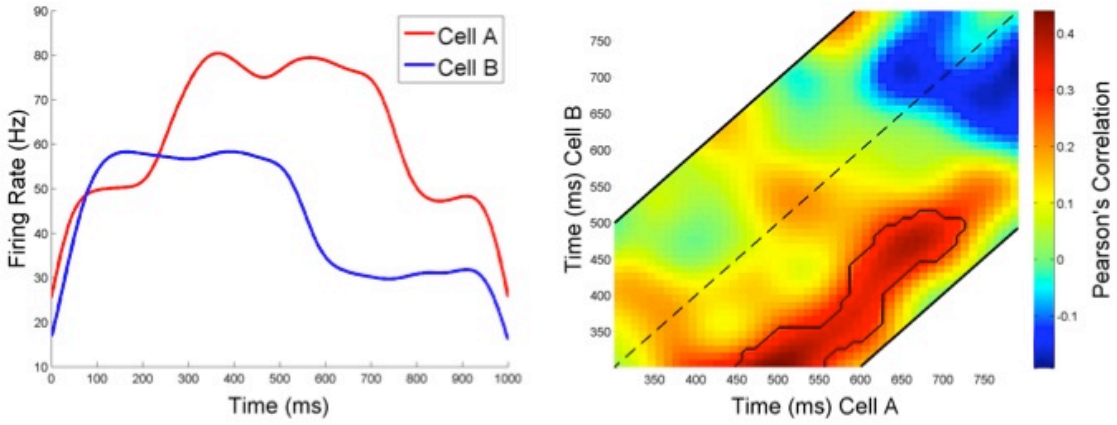

Figure Appx.3 Lagged connectivity
Connectivity between the two cells is strong, however the common input arrives at cell B 250ms before it arrives at cell A. This would simulate information flow from cell B to cell A, which is seen as a significant correlation in the lower right section of the AEC plot.

Application

For use with ECoG data, the band pass filtered applied in the frequency domain was 70-110Hz square filter with sigmoid flanks (half amplitude roll off of 1.5Hz) that also Hilbert transformed the signal (frequencies below 0Hz were set to 0

amplitude, and those above 0Hz were doubled) (Figure Appx.4). After the inverse Fourier transform was applied, and the absolute value was taken and smoothed with a moving average (100ms long) to obtain the amplitude envelope of the signal.

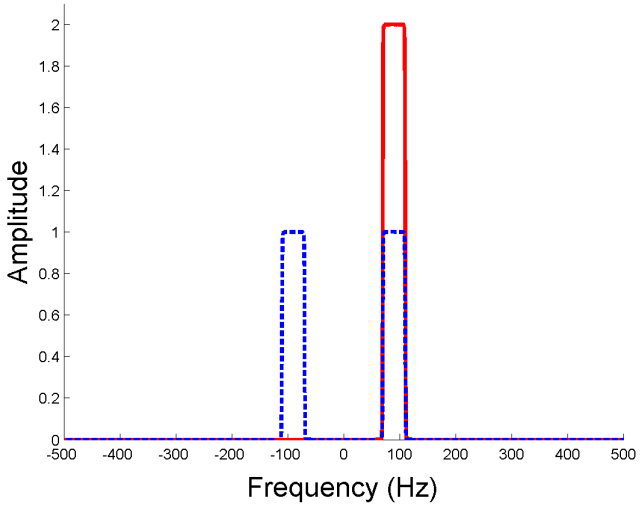

Figure Appx.4 Filter design
Two filters are shown, one is the 70-110Hz band-pass without the Hilbert transform (blue dotted line) and another with it incorporated (red solid line). Both filters are shown for a signal collected at 1kHz. The filter shape is square with sigmoid flanks, with a 3Hz half-amplitude roll-off.

REFERENCES

1. Conner, C. R., G. Chen, T. A. Pieters, and N. Tandon. 2013. Category Specific Spatial Dissociations of Parallel Processes Underlying Visual Naming. Cereb Cortex [Epub ahead of print].
2. Damasio, A. R. 1989. Time-locked multiregional retroactivation: a systems-level proposal for the neural substrates of recall and recognition. Cognition 33:25-62.
3. Glaser, W. R. 1992. Picture naming. Cognition 42:61-105.
4. Levelt, W. J. 1992. Accessing words in speech production: stages, processes and representations. Cognition 42:1-22.
5. Levelt, W. J. 2001. Spoken word production: a theory of lexical access. Proc Natl Acad Sci U S A 98:13464-13471.
6. Altmann, G. T. 1997. The Ascent of Babel. Oxford University Press, New York, New York.
7. Elman, J. L. 2004. An alternative view of the mental lexicon. Trends Cogn Sci 8:301-306.
8. Forster, K. I. 1976. Accessing the Mental Lexicon. In New Approaches to Language Mechanisms. R. J. Wales, and E. Walker, editors, Amsterdam, North-Holland. 257-287.
9. Collins, A. M., and M. R. Quillian. 1969. Retrieval time from semantic memory. J Verb Learn Verb Be 8:240-247.

10. Conrad, C. 1972. Cognitive economy in semantic memory. J Exp Psychol 92:149-155.

11. Dell, G. S., F. Chang, and Z. M. Griffin. 1999. Connectionist Models of Language Production: Lexical Access and Grammatical Encoding Cogntive Science 24:517-542.

12. Dell, G. S., and P. G. O'Seaghdha. 1992. Stages of lexical access in language production. Cognition 42:287-314.

13. Dell, G. S., M. F. Schwartz, N. Martin, E. M. Saffran, and D. A. Gagnon. 1997. Lexical access in aphasic and nonaphasic speakers. Psychol Rev 104:801-838.

14. Caramazza, A. 1997. How many levels of processing are there in Lexical Access? Cogn Neuropsychol 14:177-208.

15. Levelt, W. J., A. Roelofs, and A. S. Meyer. 1999. A theory of lexical access in speech production. Behav Brain Sci 22:1-38; discussion 38-75.

16. Roelofs, A. 1992. A spreading-activation theory of lemma retrieval in speaking. Cognition 42:107-142.

17. Bock, K., and W. J. M. Levelt. 1994. Language production : Grammatical encoding. In Handbook of Psycholinguistics. M. A. Gernsbacher, editor. Academic Press, San Diego.

18. Collins, A. M., and E. F. Loftus. 1975. A Spreading Activation Theory of Semantic Processing. Psychol Rev 82:407-428.

19. Levelt, W. J. 1999. Models of word production. Trends Cogn Sci 3:223-232.

20. Pulvermuller, F. 1999. Words in the brain's language. Behav Brain Sci 22:253-279; discussion 280-336.

21. Huyck, C. R. 2007. Creating hierarchical categories using cell assemblies. Connection Science 19:1-24.

22. Wennekers, T., M. Garagnani, and F. Pulvermuller. 2006. Language models based on Hebbian cell assemblies. J Physiol Paris 100:16-30.

23. Caramazza, A., and B. Z. Mahon. 2003. The organization of conceptual knowledge: the evidence from category-specific semantic deficits. Trends Cogn Sci 7:354-361.

24. Rapp, B., and A. Caramazza. 2002. Selective difficulties with spoken nouns and written verbs: A single case study J Neurolinguistics 15:373-402.

25. Dell, G. S. 1986. A spreading-activation theory of retrieval in sentence production. Psychol Rev 93:283-321.

26. Dell, G. S., N. Nozari, and G. M. Oppenheim. 1991. Word Production: Behavioral and Computational Considerations. In The Oxford Handbook of Language Production. V. Ferreira, M. Goldrick, and M. Miozzo, editors.

27. Pulvermuller, F. 2001. Brain reflections of words and their meaning. Trends Cogn Sci 5:517-524.

28. Pulvermuller, F., O. Hauk, V. V. Nikulin, and R. J. Ilmoniemi. 2005. Functional links between motor and language systems. Eur J Neurosci 21:793-797.

29. Pulvermuller, F., W. Lutzenberger, and H. Preissl. 1999. Nouns and verbs in the intact brain: evidence from event-related potentials and high-frequency cortical responses. Cereb Cortex 9:497-506.

30. Pulvermuller, F. 2005. Brain mechanisms linking language and action. Nat Rev Neurosci 6:576-582.

31. Pulvermuller, F., and L. Fadiga. 2010. Active perception: sensorimotor circuits as a cortical basis for language. Nat Rev Neurosci 11:351-360.

32. Oliveri, M., C. Finocchiaro, K. Shapiro, M. Gangitano, A. Caramazza, and A. Pascual-Leone. 2004. All talk and no action: a transcranial magnetic stimulation study of motor cortex activation during action word production. J Cogn Neurosci 16:374-381.

33. Mahon, B. Z., and A. Caramazza. 2008. A critical look at the embodied cognition hypothesis and a new proposal for grounding conceptual content. J Physiol Paris 102:59-70.

34. Shapiro, K., and A. Caramazza. 2003. The representation of grammatical categories in the brain. Trends Cogn Sci 7:201-206.

35. Shapiro, K. A., L. R. Moo, and A. Caramazza. 2006. Cortical signatures of noun and verb production. Proc Natl Acad Sci U S A 103:1644-1649.

36. Mahon, B. Z., S. Anzellotti, J. Schwarzbach, M. Zampini, and A. Caramazza. 2009. Category-specific organization in the human brain does not require visual experience. Neuron 63:397-405.

37. Mahon, B. Z., and A. Caramazza. 2011. What drives the organization of object knowledge in the brain? Trends Cogn Sci 15:97-103.

38. Damasio, H., T. J. Grabowski, D. Tranel, R. D. Hichwa, and A. R. Damasio. 1996. A neural basis for lexical retrieval. Nature 380:499-505.

39. Dell, G. S., L. K. Burger, and W. R. Svec. 1997. Language production and serial order: a functional analysis and a model. Psychol Rev 104:123-147.

40. Levelt, W. J. 1983. Monitoring and self-repair in speech. Cognition 14:41-104.

41. Seidenberg, M. S. 2005. Connectionist models of word reading. Curr Dir Psychol 14.

42. Seidenberg, M. S., and J. L. McClelland. 1989. A distributed, developmental model of word recognition and naming. Psychol Rev 96:523.

43. Seidenberg, M. S. 2007. Connectionist Models of Reading. In Oxford Handbook of Psycholinguistics. G. Gaskell, editor. Oxford Univeristy Press, New York, New York. 235-250.

44. Seidenberg, M. S., and J. L. McClelland. 1990. More words but still no lexicon: Reply to Besner et al.(1990). Psychol Res 97:477-452.

45. Schade, U., and T. Berg. 1992. The role of inhibition in a spreading-activation model of language production. II. The simulational perspective. J Psycholinguist Res 21:435-462.

46. Howard, D., L. Nickels, M. Coltheart, and J. Cole-Virtue. 2006. Cumulative semantic inhibition in picture naming: Experimental and computational studies. Cognition 100:464-482.

47. Berg, T., and U. Schade. 1992. The role of inhibition in a spreading-activation model of language production. I. The psycholinguistic perspective. J Psycholinguist Res 21:405-434.

48. Damasio, A. R., and D. Tranel. 1993. Nouns and verbs are retrieved with differently distributed neural systems. Proc Natl Acad Sci U S A 90:4957-4960.

49. Tranel, D., C. G. Logan, R. J. Frank, and A. R. Damasio. 1997. Explaining category-related effects in the retrieval of conceptual and lexical knowledge for concrete entities: operationalization and analysis of factors. Neuropsychologia 35:1329-1339.

50. Amunts, K., M. Lenzen, A. D. Friederici, A. Schleicher, P. Morosan, N. Palomero-Gallagher, and K. Zilles. 2010. Broca's region: novel organizational principles and multiple receptor mapping. PLoS Biol 8.

51. Poldrack, R. A., A. D. Wagner, M. W. Prull, J. E. Desmond, G. H. Glover, and J. D. Gabrieli. 1999. Functional specialization for semantic and phonological processing in the left inferior prefrontal cortex. Neuroimage 10:15-35.

52. Amunts, K., A. Schleicher, A. Ditterich, and K. Zilles. 2003. Broca's region: cytoarchitectonic asymmetry and developmental changes. J Comp Neurol 465:72-89.

53. Amunts, K., A. Schleicher, U. Burgel, H. Mohlberg, H. B. Uylings, and K. Zilles. 1999. Broca's region revisited: cytoarchitecture and intersubject variability. J Comp Neurol 412:319-341.

54. Badre, D., and A. D. Wagner. 2007. Left ventrolateral prefrontal cortex and the cognitive control of memory. Neuropsychologia 45:2883-2901.

55. Gold, B. T., D. A. Balota, S. J. Jones, D. K. Powell, C. D. Smith, and A. H. Andersen. 2006. Dissociation of automatic and strategic lexical-semantics:

functional magnetic resonance imaging evidence for differing roles of multiple frontotemporal regions. J Neurosci 26:6523-6532.

56. Gold, B. T., and R. L. Buckner. 2002. Common prefrontal regions coactivate with dissociable posterior regions during controlled semantic and phonological tasks. Neuron 35:803-812.

57. Hagoort, P. 2005. On Broca, brain, and binding: a new framework. Trends Cogn Sci 9:416-423.

58. Badre, D., R. A. Poldrack, E. J. Pare-Blagoev, R. Z. Insler, and A. D. Wagner. 2005. Dissociable controlled retrieval and generalized selection mechanisms in ventrolateral prefrontal cortex. Neuron 47:907-918.

59. Costafreda, S. G., C. H. Fu, L. Lee, B. Everitt, M. J. Brammer, and A. S. David. 2006. A systematic review and quantitative appraisal of fMRI studies of verbal fluency: role of the left inferior frontal gyrus. Hum Brain Mapp 27:799-810.

60. Gough, P. M., A. C. Nobre, and J. T. Devlin. 2005. Dissociating linguistic processes in the left inferior frontal cortex with transcranial magnetic stimulation. J Neurosci 25:8010-8016.

61. Heim, S., S. B. Eickhoff, and K. Amunts. 2008. Specialisation in Broca's region for semantic, phonological, and syntactic fluency? Neuroimage 40:1362-1368.

62. Heim, S., S. B. Eickhoff, and K. Amunts. 2009. Different roles of cytoarchitectonic BA 44 and BA 45 in phonological and semantic verbal fluency as revealed by dynamic causal modelling. Neuroimage 48:616-624.

63. Badre, D., J. Hoffman, J. W. Cooney, and M. D'Esposito. 2009. Hierarchical cognitive control deficits following damage to the human frontal lobe. Nat Neurosci 12:515-522.

64. Koechlin, E., and C. Summerfield. 2007. An information theoretical approach to prefrontal executive function. Trends Cogn Sci 11:229-235.

65. Koechlin, E., and T. Jubault. 2006. Broca's area and the hierarchical organization of human behavior. Neuron 50:963-974.

66. Sakai, K., and R. E. Passingham. 2006. Prefrontal set activity predicts rule-specific neural processing during subsequent cognitive performance. J Neurosci 26:1211-1218.

67. Pulvermuller, F. 2010. Brain-Language Research: Where is the Progress? . Biolinguistics 4:255-288.

68. Conner, C. R., T. M. Ellmore, T. A. Pieters, M. A. Disano, and N. Tandon. 2011. Variability of the Relationship between Electrophysiology and BOLD-fMRI across Cortical Regions in Humans. J Neurosci 31:12855-12865.

69. Ishai, A., L. G. Ungerleider, A. Martin, J. L. Schouten, and J. V. Haxby. 1999. Distributed representation of objects in the human ventral visual pathway. Proc Natl Acad Sci U S A 96:9379-9384.

70. Schwarzlose, R. F., J. D. Swisher, S. Dang, and N. Kanwisher. 2008. The distribution of category and location information across object-selective regions in human visual cortex. Proc Natl Acad Sci U S A 105:4447-4452.

71. Bentin, S., T. Allison, A. Puce, E. Perez, and G. McCarthy. 1996. Electrophysiological Studies of Face Perception in Humans. J Cogn Neurosci 8:551-565.

72. Haxby, J. V., M. I. Gobbini, M. L. Furey, A. Ishai, J. L. Schouten, and P. Pietrini. 2001. Distributed and overlapping representations of faces and objects in ventral temporal cortex. Science 293:2425-2430.

73. Caramazza, A., and A. E. Hillis. 1991. Lexical organization of nouns and verbs in the brain. Nature 349:788-790.

74. Tranel, D., R. Adolphs, H. Damasio, and A. R. Damasio. 2001. A neural basis for the retrieval of words for actions. Cogn Neuropsychol 18:655-674.

75. Soros, P., K. Cornelissen, M. Laine, and R. Salmelin. 2003. Naming actions and objects: cortical dynamics in healthy adults and in an anomic patient with a dissociation in action/object naming. Neuroimage 19:1787-1801.

76. Liljestrom, M., A. Hulten, L. Parkkonen, and R. Salmelin. 2009. Comparing MEG and fMRI views to naming actions and objects. Hum Brain Mapp 30:1845-1856.

77. Sahin, N. T., S. Pinker, and E. Halgren. 2006. Abstract grammatical processing of nouns and verbs in Broca's area: evidence from fMRI. Cortex 42:540-562.

78. Liljestrom, M., A. Tarkiainen, T. Parviainen, J. Kujala, J. Numminen, J. Hiltunen, M. Laine, and R. Salmelin. 2008. Perceiving and naming actions and objects. Neuroimage 41:1132-1141.

79. Goodale, M. A., and A. D. Milner. 1992. Separate visual pathways for perception and action. Trends Neurosci 15:20-25.

80. Chang, E. F., J. W. Rieger, K. Johnson, M. S. Berger, N. M. Barbaro, and R. T. Knight. 2011. Categorical speech representation in human superior temporal gyrus. Nat Neurosci 13:1428-1432.

81. Engel, A. K., C. K. Moll, I. Fried, and G. A. Ojemann. 2005. Invasive recordings from the human brain: clinical insights and beyond. Nat Rev Neurosci 6:35-47.

82. Vidal, J. R., T. Ossandon, K. Jerbi, S. S. Dalal, L. Minotti, P. Ryvlin, P. Kahane, and J. P. Lachaux. 2010. Category-Specific Visual Responses: An Intracranial Study Comparing Gamma, Beta, Alpha, and ERP Response Selectivity. Front Hum Neurosci 4:195.

83. Ojemann, G., J. Ojemann, E. Lettich, and M. Berger. 1989. Cortical language localization in left, dominant hemisphere. An electrical stimulation mapping investigation in 117 patients. J Neurosurg 71:316-326.

84. Xiong, J., S. Rao, P. Jerabek, F. Zamarripa, M. Woldorff, J. Lancaster, and P. T. Fox. 2000. Intersubject variability in cortical activations during a complex language task. Neuroimage 12:326-339.

85. Chen, G., Z. S. Saad, A. R. Nath, M. S. Beauchamp, and R. W. Cox. 2011. FMRI group analysis combining effect estimates and their variances. Neuroimage 60:747-765.

86. Price, C. J., J. T. Devlin, C. J. Moore, C. Morton, and A. R. Laird. 2005. Meta-analyses of object naming: effect of baseline. Hum Brain Mapp 25:70-82.

87. Conner, C. R., T. M. Ellmore, M. A. Disano, T. A. Pieters, A. W. Potter, and N. Tandon. 2011. Anatomic and electro-physiologic connectivity of the language system: A combined DTI-CCEP study. Comput Biol Med.

88. Swann, N. C., W. Cai, C. R. Conner, T. A. Pieters, M. P. Claffey, J. S. George, A. R. Aron, and N. Tandon. 2012. Roles for the pre-supplementary motor area and the right inferior frontal gyrus in stopping action: electrophysiological responses and functional and structural connectivity. Neuroimage 59:2860-2870.

89. Kaplan, E., H. Goodglass, and S. Weintraub. 1983. The Boston Naming Test. Lea and Febiger, Philadelphia.

90. Snodgrass, J. G., and M. Vanderwart. 1980. A standardized set of 260 pictures: norms for name agreement, image agreement, familiarity, and visual complexity. Journal of Experimental Psychology: Human Learning & Memory 6:174-215.

91. Oldfield, R. C. 1971. The assessment and analysis of handedness: the Edinburgh inventory. Neuropsychologia 9:97-113.

92. Salmelin, R., R. Hari, O. V. Lounasmaa, and M. Sams. 1994. Dynamics of brain activation during picture naming. Nature 368:463-465.

93. Cox, R. W. 1996. AFNI: software for analysis and visualization of functional magnetic resonance neuroimages. Comput Biomed Res 29:162-173.

94. Dale, A. M., B. Fischl, and M. I. Sereno. 1999. Cortical surface-based analysis. I. Segmentation and surface reconstruction. Neuroimage 9:179-194.

95. Wada, J., and T. Rasmussen. 2007. Intracarotid injection of sodium amytal for the lateralization of cerebral speech dominance. 1960. J Neurosurg 106:1117-1133.

96. Tandon, N. 2012. Mapping of Human Language. In Clinical Brain Mapping. D. Yoshor, editor. McGraw Hill.

97. Pieters, T. A., C. R. Conner, and N. Tandon. 2013. Recursive grid partitioning on a cortical surface model: an optimized technique for the localization of implanted subdural electrodes. J Neurosurg.

98. Viechtbauer, W. 2010. Conducting meta-analyses in R with the metafor package. Journal of Statistical Software 36:1-48.

99. Acar, Z. A., J. Palmer, G. Worrell, and S. Makeig. 2011. Electrocortical source imaging of intracranial EEG data in epilepsy. Conf Proc IEEE Eng Med Biol Soc 2011:3909-3912.

100. Friston, K. J., A. P. Holmes, C. J. Price, C. Buchel, and K. J. Worsley. 1999. Multisubject fMRI studies and conjunction analyses. Neuroimage 10:385-396.

101. Szekely, A., S. D'Amico, A. Devescovi, K. Federmeier, D. Herron, G. Iyer, T. Jacobsen, A. L. Arevalo, A. Vargha, and E. Bates. 2005. Timed action and object naming. Cortex 41:7-25.

102. Brysbaert, M., and B. New. 2009. Moving beyond Kucera and Francis: a critical evaluation of current word frequency norms and the introduction of a

new and improved word frequency measure for American English. Behav Res Methods 41:977-990.

103. Indefrey, P., and W. J. Levelt. 2004. The spatial and temporal signatures of word production components. Cognition 92:101-144.

104. Luders, H., R. P. Lesser, J. Hahn, D. S. Dinner, H. H. Morris, E. Wyllie, and J. Godoy. 1991. Basal temporal language area. Brain 114 (Pt 2):743-754.

105. Kanwisher, N. 2010. Functional specificity in the human brain: a window into the functional architecture of the mind. Proc Natl Acad Sci U S A 107:11163-11170.

106. Wise, R. J., J. Greene, C. Buchel, and S. K. Scott. 1999. Brain regions involved in articulation. Lancet 353:1057-1061.

107. Acar, Z. A., S. Makeig, and G. Worrell. 2008. Head modeling and cortical source localization in epilepsy. Conf Proc IEEE Eng Med Biol Soc 2008:3763-3766.

108. Saad, Z. S., and R. C. Reynolds. 2012. SUMA. Neuroimage 62:768-773.

109. Saad, Z. S., S. J. Gotts, K. Murphy, G. Chen, H. J. Jo, A. Martin, and R. W. Cox. 2012. Trouble at rest: how correlation patterns and group differences become distorted after global signal regression. Brain Connect 2:25-32.

110. Martin, A., J. V. Haxby, F. M. Lalonde, C. L. Wiggs, and L. G. Ungerleider. 1995. Discrete cortical regions associated with knowledge of color and knowledge of action. Science 270:102-105.

111. Rizzolatti, G., and M. Matelli. 2003. Two different streams form the dorsal visual system: anatomy and functions. Exp Brain Res 153:146-157.

112. Ungerleider, L. G., and J. V. Haxby. 1994. 'What' and 'where' in the human brain. Curr Opin Neurobiol 4:157-165.

113. Edwards, E., S. S. Nagarajan, S. S. Dalal, R. T. Canolty, H. E. Kirsch, N. M. Barbaro, and R. T. Knight. 2010. Spatiotemporal imaging of cortical activation during verb generation and picture naming. Neuroimage 50:291-301.

114. Petrides, M. 2000. The role of the mid-dorsolateral prefrontal cortex in working memory. Exp Brain Res 133:44-54.

115. MacDonald, A. W., 3rd, J. D. Cohen, V. A. Stenger, and C. S. Carter. 2000. Dissociating the role of the dorsolateral prefrontal and anterior cingulate cortex in cognitive control. Science 288:1835-1838.

116. du Boisgueheneuc, F., R. Levy, E. Volle, M. Seassau, H. Duffau, S. Kinkingnehun, Y. Samson, S. Zhang, and B. Dubois. 2006. Functions of the left superior frontal gyrus in humans: a lesion study. Brain 129:3315-3328.

117. Hickok, G. 2012. Computational neuroanatomy of speech production. Nat Rev Neurosci 13:135-145.

118. Lachaux, J. P., E. Rodriguez, J. Martinerie, and F. J. Varela. 1999. Measuring phase synchrony in brain signals. Hum Brain Mapp 8:194-208.

119. Korzeniewska, A., P. J. Franaszczuk, C. M. Crainiceanu, R. Kus, and N. E. Crone. 2011. Dynamics of large-scale cortical interactions at high gamma frequencies during word production: Event related causality (ERC) analysis of human electrocorticography (ECoG). Neuroimage.

120. Adhikari, A., T. Sigurdsson, M. A. Topiwala, and J. A. Gordon. 2010. Cross-correlation of instantaneous amplitudes of field potential oscillations: a straightforward method to estimate the directionality and lag between brain areas. J Neurosci Methods 191:191-200.

121. Wada, J., and T. B. Rasmussen. 1960. Intracarotid injection of sodium amytal for the lateralization of cerebral speech dominance. J Neurosurg 17:166-282.

122. Bruns, A., R. Eckhorn, H. Jokeit, and A. Ebner. 2000. Amplitude envelope correlation detects coupling among incoherent brain signals. Neuroreport 11:1509-1514.

123. Hipp, J. F., D. J. Hawellek, M. Corbetta, M. Siegel, and A. K. Engel. 2012. Large-scale cortical correlation structure of spontaneous oscillatory activity. Nat Neurosci.

124. Nir, Y., R. Mukamel, I. Dinstein, E. Privman, M. Harel, L. Fisch, H. Gelbard-Sagiv, S. Kipervasser, F. Andelman, M. Y. Neufeld, U. Kramer, A. Arieli, I. Fried, and R. Malach. 2008. Interhemispheric correlations of slow spontaneous neuronal fluctuations revealed in human sensory cortex. Nat Neurosci 11:1100-1108.

125. Sporns, O. 2010. Networks of the Brain. MIT Press.

126. Rousseeuw, P. J. 1987. A graphical aid to the interpretation and validation of cluster analysis. J Comput Appl Math 20:53-65.

127. Ramot, M., L. Fisch, M. Harel, S. Kipervasser, F. Andelman, M. Y. Neufeld, U. Kramer, I. Fried, and R. Malach. 2012. A widely distributed spectral signature

of task-negative electrocorticography responses revealed during a visuomotor task in the human cortex. J Neurosci 32:10458-10469.

128. Snyder, H. R., N. Hutchison, E. Nyhus, T. Curran, M. T. Banich, R. C. O'Reilly, and Y. Munakata. 2010. Neural inhibition enables selection during language processing. Proc Natl Acad Sci U S A 107:16483-16488.

129. Kitano, H. 2004. Biological robustness. Nat Rev Genet 5:826-837.

130. Dronkers, N. F. 1996. A new brain region for coordinating speech articulation. Nature 384:159-161.

131. Sakai, K., and R. E. Passingham. 2003. Prefrontal interactions reflect future task operations. Nat Neurosci 6:75-81.

132. Badre, D., and M. D'Esposito. 2009. Is the rostro-caudal axis of the frontal lobe hierarchical? Nat Rev Neurosci 10:659-669.

133. Heim, S., S. B. Eickhoff, A. K. Ischebeck, A. D. Friederici, K. E. Stephan, and K. Amunts. 2009. Effective connectivity of the left BA 44, BA 45, and inferior temporal gyrus during lexical and phonological decisions identified with DCM. Hum Brain Mapp 30:392-402.

134. Lachaux, J. P., E. Rodriguez, J. Martinerie, C. Adam, D. Hasboun, and F. J. Varela. 2000. A quantitative study of gamma-band activity in human intracranial recordings triggered by visual stimuli. Eur J Neurosci 12:2608-2622.

135. Watrous, A. J., N. Tandon, C. R. Conner, T. Pieters, and A. D. Ekstrom. 2013. Frequency-specific network connectivity increases underlie accurate spatiotemporal memory retrieval. Nat Neurosci.

136. Canolty, R. T., K. Ganguly, S. W. Kennerley, C. F. Cadieu, K. Koepsell, J. D. Wallis, and J. M. Carmena. 2010. Oscillatory phase coupling coordinates anatomically dispersed functional cell assemblies. Proc Natl Acad Sci U S A 107:17356-17361.

137. Miller, K. J., D. Hermes, C. J. Honey, M. Sharma, R. P. Rao, M. den Nijs, E. E. Fetz, T. J. Sejnowski, A. O. Hebb, J. G. Ojemann, S. Makeig, and E. C. Leuthardt. 2010. Dynamic modulation of local population activity by rhythm phase in human occipital cortex during a visual search task. Front Hum Neurosci 4:197.

138. Buzsaki, G. 2004. Large-scale recording of neuronal ensembles. Nat Neurosci 7:446-451.

139. Mitzdorf, U. 1985. Current source-density method and application in cat cerebral cortex: investigation of evoked potentials and EEG phenomena. Physiol Rev 65:37-100.

140. Swann, N., H. Poizner, M. Houser, S. Gould, I. Greenhouse, W. Cai, J. Strunk, J. George, and A. R. Aron. 2011. Deep brain stimulation of the subthalamic nucleus alters the cortical profile of response inhibition in the beta frequency band: a scalp EEG study in Parkinson's disease. J Neurosci 31:5721-5729.

141. Buzsáki, G. 2006. Rhythms of the Brain. Oxford University Press, Oxford.

142. Friederici, A. D. 2006. What's in control of language? Nat Neurosci 9:991-992.

143. Friston, K. 2009. Causal modelling and brain connectivity in functional magnetic resonance imaging. PLoS Biol 7:e33.

144. Friston, K. J., L. Harrison, and W. Penny. 2003. Dynamic causal modelling. Neuroimage 19:1273-1302.

145. Kiebel, S. J., O. David, and K. J. Friston. 2006. Dynamic causal modelling of evoked responses in EEG/MEG with lead field parameterization. Neuroimage 30:1273-1284.

146. Damasio, H., T. J. Grabowski, D. Tranel, L. L. Ponto, R. D. Hichwa, and A. R. Damasio. 2001. Neural correlates of naming actions and of naming spatial relations. Neuroimage 13:1053-1064.

147. Levelt, W. J., H. Schriefers, A. S. Meyer, T. Pechmann, D. Vorberg, and J. Havinga. 1991. The time course of lexical access in speech production: A study of picture naming. Psychological Review 98:122-142.

148. Binder, J. R., and R. H. Desai. 2011. The neurobiology of semantic memory. Trends Cogn Sci 15:527-536.

149. Binder, J. R., R. H. Desai, W. W. Graves, and L. L. Conant. 2009. Where is the semantic system? A critical review and meta-analysis of 120 functional neuroimaging studies. Cereb Cortex 19:2767-2796.

150. Buchel, C., C. Price, and K. Friston. 1998. A multimodal language region in the ventral visual pathway. Nature 394:274-277.

151. Snyder, H. R., M. T. Banich, and Y. Munakata. 2011. Choosing our words: retrieval and selection processes recruit shared neural substrates in left ventrolateral prefrontal cortex. J Cogn Neurosci 23:3470-3482.

152. Tandon, N., editor. 2008. Cortical Mapping by Electrical Stimulation of Subdural Electrodes: Language areas.

153. Logothetis, N. K., M. Augath, Y. Murayama, A. Rauch, F. Sultan, J. Goense, A. Oeltermann, and H. Merkle. 2010. The effects of electrical microstimulation on cortical signal propagation. Nat Neurosci 13:1283-1291.

154. Nir, Y., I. Dinstein, R. Malach, and D. J. Heeger. 2008. BOLD and spiking activity. Nat Neurosci 11:523-524; author reply 524.

155. Towle, V. L., H. A. Yoon, M. Castelle, J. C. Edgar, N. M. Biassou, D. M. Frim, J. P. Spire, and M. H. Kohrman. 2008. ECoG gamma activity during a language task: differentiating expressive and receptive speech areas. Brain 131:2013-2027.

156. Cervenka, M. C., J. Corines, D. F. Boatman-Reich, A. Eloyan, X. Sheng, P. J. Franaszczuk, and N. E. Crone. 2012. Electrocorticographic functional mapping identifies human cortex critical for auditory and visual naming. Neuroimage.

157. Crone, N. E., D. Boatman, B. Gordon, and L. Hao. 2001. Induced electrocorticographic gamma activity during auditory perception. Brazier Award-winning article, 2001. Clin Neurophysiol 112:565-582.

158. Crone, N. E., L. Hao, B. J. Hart, D. Boatman, R. P. Lesser, R. Irizarry, and B. Gordon. 2001. Electrocorticographic gamma activity during word production in spoken and sign language. Neurology 57:2045-2053.

159. Crone, N. E., D. L. Miglioretti, B. Gordon, and R. P. Lesser. 1998. Functional mapping of human sensorimotor cortex with electrocorticographic spectral

analysis. II. Event-related synchronization in the gamma band. Brain 121 (Pt 12):2301-2315.

160. Mesgarani, N., and E. F. Chang. 2012. Selective cortical representation of attended speaker in multi-talker speech perception. Nature 485:233-236.

161. Keller, C. J., S. Bickel, C. J. Honey, D. M. Groppe, L. Entz, R. C. Craddock, F. A. Lado, C. Kelly, M. Milham, and A. D. Mehta. 2013. Neurophysiological Investigation of Spontaneous Correlated and Anticorrelated Fluctuations of the BOLD Signal. J Neurosci 33:6333-6342.

162. Canolty, R. T., E. Edwards, S. S. Dalal, M. Soltani, S. S. Nagarajan, H. E. Kirsch, M. S. Berger, N. M. Barbaro, and R. T. Knight. 2006. High gamma power is phase-locked to theta oscillations in human neocortex. Science 313:1626-1628.

163. Mantini, D., M. G. Perrucci, C. Del Gratta, G. L. Romani, and M. Corbetta. 2007. Electrophysiological signatures of resting state networks in the human brain. Proc Natl Acad Sci U S A 104:0027-8424.

164. Fox, M. D., and M. E. Raichle. 2007. Spontaneous fluctuations in brain activity observed with functional magnetic resonance imaging. Nature Reviews Neuroscience 8:1471-1003X.

165. Fox, M. D., M. Corbetta, A. Z. Snyder, J. L. Vincent, and M. E. Raichle. 2006. Spontaneous neuronal activity distinguishes human dorsal and ventral attention systems. Proc Natl Acad Sci U S A 103:0027-8424.

166. Dayan, P., and L. F. Abbott. 2001. Theoretical Neuroscience: Computational and Mathematical Modeling of Neural Systems. MIT Press, Cambridge, Massachusetts.

167. Gabbiani, F., and S. J. Cox. 2010. Mathematics for Neuroscientists. Elsevier, Burlington, MA.

VITA

Christopher Richard Conner was born in Great Falls, Montana on September 3, 1985, the son of Susan and Christopher Conner. After completing his work at Charles M. Russell High School in 2004, he entered Rice University in Houston, Texas. He received the degree of Bachelor of Arts with a major in Computational and Applied Mathematics in May, 2008. That fall, he began medical at The University of Texas at Houston. He completed two years of medical school before beginning his PhD studies in Neuroscience at The University of Texas Health Science Center at Houston Graduate School of Biomedical Sciences.

Permanent address:
2600 Bellefontaine St, Apt D19
Houston, TX 77025